Design, Implementation and Control of Self-Aligning, Bowden Cable-Driven, Series Elastic Exoskeletons for Lower Extremity Rehabilitation

by

Beşir Çelebi

Submitted to the Graduate School of Sabancı University
in partial fulfillment of the requirements for the degree of
Master of Science

Sabancı University

August, 2013

Design, Implementation and Control of

Self-Aligning, Bowden Cable-Driven, Series Elastic Exoskeletons

for Lower Extremity Rehabilitation

APPROVED BY:

Assoc. Prof. Dr. Volkan Patoğlu   ....
(Thesis Advisor)

Assoc. Prof. Dr. Güllü Kızıltaş Şendur   ....

Assoc. Prof. Dr. Kemalettin Erbatur   ....
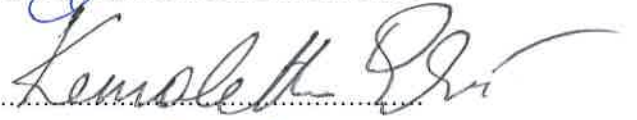
Assist. Prof. Dr. Murat Yeşiloglu   ....

Dr. Emre Özlü   ....

DATE OF APPROVAL: 13. 08. 2013

Design, Implementation and Control of Self-Aligning, Bowden Cable-Driven, Series Elastic Exoskeletons for Lower Extremity Rehabilitation

Beşir Çelebi

Mechatronics Engineering, Master of Science, 2013

Thesis Supervisor: Assoc. Prof. Dr. Volkan Patoğlu

Abstract

We present AssistOn-Leg, a modular, self-aligning exoskeleton for robot-assisted rehabilitation of lower extremities. AssistOn-Leg consists of three self-aligning, powered exoskeletons targeting ankle, knee and hip joints, respectively. Each module can be used in a stand-alone manner to provide therapy to its corresponding joint or the modules can be connected together to deliver natural gait training to patients. In particular, AssistOn-Ankle targets dorsiflexion/plantarflexion and supination/pronation of human ankle and can be configured to deliver balance/proprioception or range of motion/strengthening exercises; AssistOn-Knee targets flexion/extension movements of the knee joint, while also accommodating its translational movements in the sagittal plane; and AssistOn-Hip targets flexion/extension movements hip joint, while allowing for translations of hip-pelvis complex in the sagittal plane. Automatically aligning their joint axes, modules of AssistOn-Leg ensure an ideal match between human joint axes and the exoskeleton axes. Self-alignment of the modules not only guarantees ergonomy and comfort throughout the therapy, but also significantly shortens the setup time required to attach a patient to the exoskeleton.

Bowden cable-driven series elastic actuation is utilized in the modules located at the distal (knee and ankle) joints of AssistOn-Leg to keep the apparent inertia of the system low, while simultaneously providing large actuation torques required to support human gait. Series elasticity also provides good force tracking characteristics, active back-driveability within the control bandwidth and passive compliance as well as impact resistance for excitations above this bandwidth. AssistOn-Hip is designed to be passively back-driveable with a capstan-based multi-level transmission. Thanks to passive compliance of the distal modules and passive back-driveability of the hip module, the overall design ensures safety even under power losses and robustness throughout the whole frequency spectrum.

Kendini Hizalayan, Bowden Kablo Sürülü, Seri Elastik Eyleyicili Robotik Rehabilitasyon Amaçlı Alt Ekstremite Dışiskeletlerin Tasarımı, Uygulaması ve Kontrolü

Beşir Çelebi
Yüksek Lisans Tezi, 2013
Tez Danışmanı: Doç. Dr. Volkan Patoğlu

Anahtar kelimeler: Robot Destekli Rehabilitasyon, Seri-Elastik Eyleyici, Kuvvet Geri-Beslemeli Dışİskelet, Kendini Hizalama, Bowden Kablo Sürülü Eyleyici.

Özetçe

Bu çalışmada, alt ekstremitelerin robot yardımlı rehabilitasyonu amaçlı birimsel ve kendini hizalayan dışiskelet, AssistOn-Leg sunulmaktadır. AssistOn-Leg, sırasıyla ayak bileği, diz ve kalça eklemlerini hedefleyen üç kendini hizalayan ve güçlendirilmiş dışiskelet biriminden oluşmaktadır. Her bir birim bağımsız olarak ilgilendiği eklemin rehabilitasyonunda kullanılabilirken, birimlerin bir araya getirilmesiyle de doğal yürüyüş alıştırmaları gerçekleştirilebilir. AssistOn-Ankle ayak bileğinin plantar fleksiyon/dorsifleksiyon ve supinasyon/pronasyon hareketlerini hedeflemekte ve denge/propriosepsionu ya da hareket aralığı/güçlendirme alıştırmalarını verebilecek şekilde yeniden yapılandırılabilmektedir. AssistOn-Knee diz ekleminin fleksiyon/ekstensiyon hareketini hedeflemekte ve aynı anda bu harekete bağlı sagital düzlemde oluşan öteleme hareketlerini de desteklemektedir. AssistOn-Hip kalça ekleminin fleksiyon/ekstensiyon hareketini hedeflemekte ve kalça-leğen kemiği bileşiğinin sagital düzlemdeki öteleme hareketlerine izin vermektedir. Eklem eksenlerinin kendi kendine hizalanması sonucunda, AssistOn-Leg ve birimleri insan eklem eksenleri ve robot eksenleri arasında kusursuz bir eşleşmeyi garanti etmektedir. Bu sayede, kendini hizalama, terapi süresince ergonomi ve rahatlığı sağlarken cihazların kurulumu ve hastaya bağlanması için gereken süreyi de önemli ölçüde azaltmaktadır.

Bowden kablo sürülü seri elastik eyleyicilerden ayak bileği ve diz birimlerinde, insan yürüyüşünü destekleyecek yüksek eyleyici torku sağlanırken sistemin belirgin ataletinin düşük tutulması amacıyla yararlanıldı. Ayrıca seri elastiklik, iyi kuvvet takibi nitelikleri, kontrol bant genişliği içerisinde aktif geri sürülebilirlik, pasif yumuşaklık ve kontrol bant genişliği dışındaki uyarılmalara karşı darbe direnci gibi özellikleri imkan vermektedir. AssistOn-Hip tasarımında ise pasif geri sürülebilir olması amacıyla çoklu seviyeli ırgat temelli bir iletim kullanılmıştır. Ayak bileği ve diz birimlerindeki pasif yumuşaklık ve kalça birimindeki pasif geri sürülebilirlik sayesinde, genel sistem tasarımının güç kaybında bile emniyetli olması ve tüm frekans tayfında gürbüzlük garanti edilmiştir.

Acknowledgements

also Süleyman Tutkun for his precious support to work done for my research.

Finally, I would like to give my very special thanks to my mother, my sisters and my father for all their love, patience and support in all my choices. They encouraged me to overcome every difficulties I face off. I will be pleased to dedicate this thesis to them.

Contents

List of Figures

List of Tables

Chapter I

1   Introduction

Stroke is one of the major causes of loss of movement capability and annu-
ally over 15 million people suffer from stroke [7]. Physical rehabilitation is
an indispensable form of treatment in developing, maintaining and restoring
movement capabilities of those of who are injured [8]. Physical therapy is
known to be more effective if its application is repetitive [9], intense [10],
long term [11] and task specific [12]. Traditionally rehabilitation exercises
are delivered by physical therapists and effective therapies are costly due to
the amount of manual labor involved. Robotic rehabilitation is a relatively
new method of delivering physical rehabilitation that can provide repetitive
and physically involved rehabilitation exercises with increased intensity and
accuracy, while avoiding the labor related costs. In these therapies, thera-
pists oversee the process and make decisions, while they are not burdened
with physically involved exercises. Moreover, robot assisted rehabilitation
increases efficiency of therapies and can provide quantitative measurements
of patient progress. Clinical trials on robot assisted rehabilitation provide ev-
idence that this form of therapy is effective for motor recovery and possesses
high potential for improving functional independence of patients [13–16].

Much of research in the area of rehabilitation robotics has concentrated on
design of highly backdriveable and/or compliant robots for safe human-robot

interaction even under power losses [17–20] and derivation of control algorithms that assist patients only as much as needed [21–23], such that active involvement of patients in therapy routines can be ensured. Another important line of research specifically focuses on design of ergonomic exoskeleton-type rehabilitation robots. Cenciarini *et al.* indicates that exoskeletons need to be anatomically compatible with human joints in order to deliver safe and effective therapy sessions, since they are physically attached to humans [24].

Exoskeletons are preferred for rehabilitation, since, as a result of multiple interaction points with human and the exoskeleton, movement of these devices correspond with human joints and targeted joints can be controlled and measured, individually. However, matching human joint axes with robot axes is an imperative design criteria to avoid misalignments that mainly occur due to over-simplification of kinematics of human joints, difficulty in exact determination of human joint configurations and infeasibility of exact placement of human limb to the exoskeleton in between therapy sessions [25,26]. Consequently, misalignment causes parasitic forces that results in discomfort, pain or even long term injury under repetitive use. More importantly, potential recovery can be inhibited and real life use of the limb can be decreased due to unfavored energetics of compensatory movements that are promoted by axis misalignment [27].

The need for exoskeletons that can comply with complex movements of human joints has been first pointed out for the shoulder joint [28] and since then, several exoskeletons that can replicate or closely approximate complex shoulder joint movements have been proposed [6,29,30]. Complex joint movements at the lower limbs have received relatively less attention. For instance, even though most prosthetics and orthotics devices, such as [31,32],

2

enable complex movements at the knee and allow changing of joint center location during motion, this capability has not been integrated in most of the existing rehabilitation devices. Well-known lower limb exoskeletons such as Lokomat models the knee and hip joint as perfect revolute joints in the sagittal plane and other movements that exist in these joint are simply neglected [1]. Similarly, ALEX [3] and LOPES [4] model the knee joint as a perfect revolute joint, while they include mechanisms with complex kinematics to enable translations of hip and pelvis joint along with hip rotations. Even though simplified, motion of the hip-pelvic complex is considered in these designs, since the kinematic complexity and especially the range of motion (RoM) of hip is much larger than that of knee. Besides, these devices are either designed up to ankle or have passive revolute joint to enable plantar flexion/dorsiflexion. Other devices in the literature such as [2, 5, 33] have similar kinematics to the aforementioned devices. Figure 1.1 presents several examples of lower extremity exoskeletons listed above.

To ensure safety of the exoskeleton while interacting with human users, low inertia and high back-driveability are targeted. On the other hand, to maintain high torques required for assisting lower extremities, powerful actuators with large gear-ratios are necessitated, limiting the back-driveability and increasing apparent inertia of these devices. In most of the exoskeleton designs in the literature, actuators and gear trains are placed on the joints [1, 2, 5] themselves. There are also exoskeletons that make use of pneumatic actuators [3]. Lopes is unique in that, it is based on Bowden cable-driven series elastic actuation [4]. Bowden cable-drive allows actuators to be remotely located and the apparent inertia to be reduced. Series elasticity of this exoskeleton enables the device to be safe against impacts, whereas
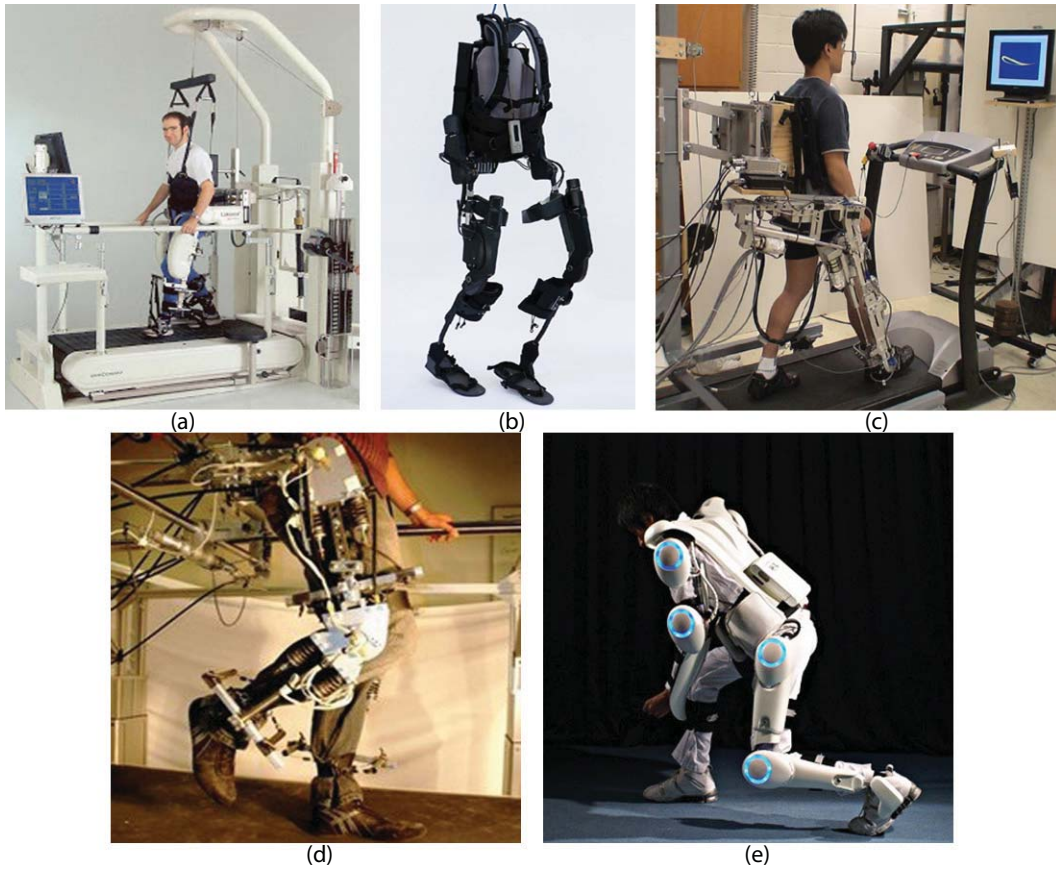
Figure 1.1: Lower extremity exoskeletons: (a) Lokomat [1], (b) eLEGS [2], (c) ALEX [3], (d) Lopes [4] and (e) HAL [5].

active back-driveability is maintained with force feedback controller. Moreover, series elasticity helps compensate the high amount and varying nature of friction available in the system due to Bowden cables.

Even though ergonomy along with safety of the user are aimed in all lower extremity exoskeleton designs, all of these rehabilitation devices model the knee joint motion as a 1 DoF hinge joint and completely neglect the complexity of ankle motions. Rolling motion at the knee joint during flexion/extension is crucial in replicating the natural human gait, while ankle

Figure 1.2: Solid model of AssistOn-Leg

push-off is one of the most important aspects of energetics of human locomotion. In this thesis, we propose a self-aligning, Bowden cable-actuated, series elastic lower extremity exoskeleton, AssistOn-Leg, that features a modular design with three modules targeting hip, knee and ankle, respectively. All of the modules of AssistOn-Leg, shown in Figure 1.2, are designed possess self-alignment feature, such that AssistOn-Leg can ideally comply with the complex kinematics of human joints by automatically aligning all its joint. Self-aligning feature of AssistOn-Leg also significantly shortens the setup time required to attach the patient to the exoskeleton. Bowden cable-driven series elastic actuation is utilized in the modules located at the distal (knee and ankle) joints of the exoskeleton to keep the apparent inertia of the system low, while simultaneously providing large actuation torques required to support human gait. Series elasticity also provides active backdriveability, good force tracking characteristics and impact resistance to AssistOn-Leg

1.1 Contributions

- ASSISTON-LEG, a modular, self-aligning, powered exoskeleton targeting ankle, knee and hip joints, is designed for physical rehabilitation of lower extremity.

  - Self-aligning feature enables the exoskeleton axes and human joint axes to perfectly match. Therefore, ASSISTON-LEG does not intervene with the natural and efficient for gait of patients and parasitic forces that cause discomfort, pain and long term injury under repetitive use are avoided.

  - Providing assistance to relevant parts of lower extremity, potential recovery is promoted.

  - Setup time required to wear the exoskeleton is significantly shortened such that therapy duration is used more effectively for rehabilitation exercises instead of being spent for adjustments of the device.

- Design and implementation of an under-actuated, self-aligning, powered knee exoskeleton has been conducted.

  - ASSISTON-KNEE actively supports flexion/extension movements of the knee joint, while also passively accommodating its translational movements in the sagittal plane.

  - Kinematics, actuation, detailed design, experimental characterization results and initial user evaluations are presented for ASSISTON-KNEE.

– Setup time is less than 1 minute whereas it takes about 10 minutes for a similar knee exoskeleton, Roboknee [44].

• Design and implementation of a reconfigurable, self-aligning, redundant, powered ankle exoskeleton, ASSISTON-ANKLE, has been completed.

  – ASSISTON-ANKLE actively targets dorsiflexion/plantarflexion and supination/pronation of human ankle and can be configured to deliver balance/proprioception or range of motion/strengthening exercises.

  – Thanks to reconfigurability of the device, RoM/strengthening exercises can be treated with the help of a 3UPS mechanism, whereas 3RPS mechanism can be used to support balance/proprioception exercises.

  – Kinematics, actuation and detailed design are presented for ASSISTON-ANKLE.

  – Setup time of ASSISTON-ANKLE is about 2 minutes.

• Bowden cable-driven series elastic actuation is implemented for the modules located at the distal (knee and ankle) joints of ASSISTON-LEG.

  – Bowden cable-drive helps keep the apparent inertia of the system low, while simultaneously providing large actuation torques required to support human gait.

  – Series elasticity effectively converts the force control problem into position control problem and enables more robust control, since

8

higher controller gains are allowed. Higher control gains are useful to compensate parasitic effects of friction, backlash and torque ripple in power transmission.

– Series elasticity provides good force tracking characteristics, active back-driveability within the control bandwidth and passive compliance as well as impact resistance for excitations above this bandwidth.

- Design of a self-aligning hip ankle exoskeleton, ASSISTON-HIP, has been proposed.

  – ASSISTON-HIP actively targets flexion/extension movements hip joint, while actively imposing or passively allowing for translations of hip-pelvis complex in the sagittal plane.

  – Passively back-driveable capstan-based multi-level transmission is proposed for the hip module.

  – Passive back-driveability ensures safety even under power losses.

  – Kinematics, actuation details and solid model are presented for ASSISTON-HIP.

1.2   Structure of the Thesis

We cover human joints at the lower extremity in an order with increasing level of complexity . Along these lines, the rest of the thesis is organized to cover as follows:

In Chapter II, design, implementation and control of the knee module AssistOn-Knee is discussed. In particular, human knee anatomy is given in Section 2.1. The kinematic type selection for this device is explained in Section 2.2 and kinematic analysis is performed in Section 2.3. Design is discussed along with implementation details in 2.4, while the controller design and experimental characterization of AssistOn-Knee is given in Section 2.5. Lastly, Section 2.6 presents user studies with the exoskeleton.

Chapter III explains design, implementation details and control of ankle exoskeleton, AssistOn-Ankle. Firstly, the anatomy of human ankle is summarized in Section 3.1. Then, the motivation and kinematic type selection for the device is explained in Section 3.2, while kinematics of ankle exoskeleton is analyzed in Section 3.3. Design and implementation details are discussed in Section 3.4, while control of AssistOn-Ankle is discussed and kinematic verification is provided in Section 3.5.

Chapter IV covers conceptual design of AssistOn-Leg and design details of the hip module AssistOn-Hip. In particular, kinematics of human hip-pelvis complex is given in Section 4.1. The need for complex movements at the hip and type selection for the hip joint are discussed in Section 4.2. Kinematics of AssistOn-Hip is derived in Section 4.3. Finally, integration of the modules to form AssistOn-Leg and design details are presented in Section 4.4.

Chapter V concludes the thesis and lists the planned future works.

Chapter II

2   ASSISTON-KNEE

This chapter presents motivation, kinematics, design, control, implementation details and user evaluations of knee exoskeleton, ASSISTON-KNEE. The chapter also covers kinematics of human knee joint.

2.1   Kinematics of Human Knee

Human knee joint, in detail, can be kinematically modeled as a 6 DoF joint [34]. But, due to limitations of strong ligaments and muscles, most of these DoFs are prohibited significantly. This allows simplified models of knee joint with less DoF to be utilized faithfully to represent knee kinematics [35]. Even though, the flexion-extension is the dominant movement in the sagittal plane of the knee, human knee can not be modeled as a true revolute joint in this plane. In particular, during flexion-extension of the knee, tibia rolls on femur resulting in anterior-posterior (AP) translations as depicted in Figure 2.1. The rolling between tibia and femur results in significant amount of AP translations, with movements exceeding 19 mm in the sagittal plane, as modeled in [36, 37] and verified in [38] using x-ray measurements of human subjects. Furthermore, AP translations are coupled to the flexion-extension rotation of the knee and the exact nature of these translations strongly depends on the on physical structure of the femur and tibia and shape of the
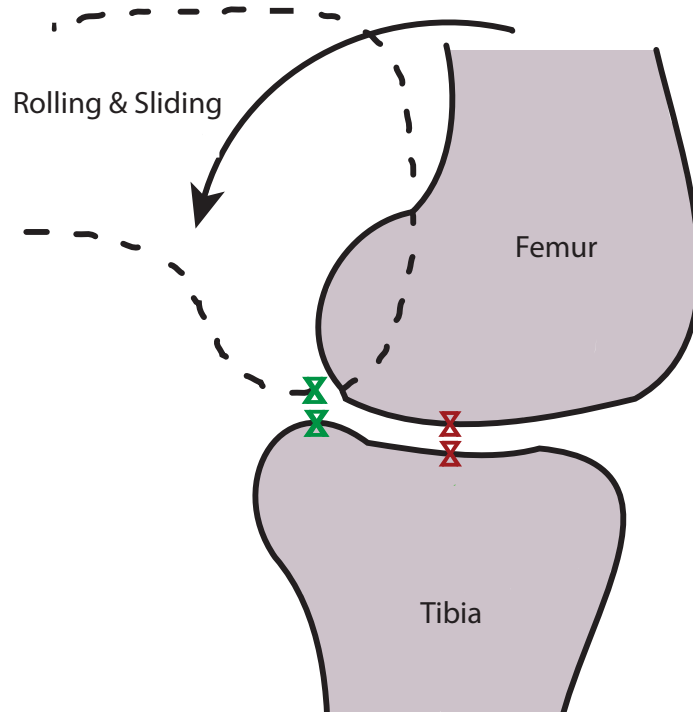
Figure 2.1: Schematic representation of sagittal plane anterior-posterior translation during flexion/extension of knee joint

articulated surfaces. As a result, this motion is unique for every individual.

In addition to the flexion-extension rotation coupled with AP translations in the sagittal plane, other significant motion of human knee joint is the internal/external rotation, with a range up to 50° when the knee is fully flexed. However, internal/external rotation of human knee is severely constrained when it is loaded under body weight or fully extended [39].

2.2 ASSISTON-KNEE

Most devices in literature models knee with one DoF for flexion/extension [3, 4, 40, 41]. Furthermore, in [42] a torsional spring based series elastic actuator is employed with a revolute joint at the knee, while in [43] a variable

stiffness actuator is used to actuate a knee exoskeleton that models knee as a perfect hinge. However, movement of knee joint cannot be modeled as simple as a perfect hinge. Pratt *et al.* have introduced a series elastic knee exoskeleton that *partially* supports AP translations of the knee joint thanks to its kinematic structure that utilizes two revolute joints in series [44]. This exoskeleton can provide assistance during both flexion/extension movements of the knee. A similar kinematic structure has also been used in [45] to partially allow AP translations, while also providing assistance during the flexion movement of the knee. Note that, both of these devices can only approximate AP transitions of the knee joint up to some degree and cannot comply with actual 3 DoF movements of the knee taking place in the sagittal plane.

More recently, several exoskeletons that enable coupled AP translation of the knee joint along with flexion-extension movements have been introduced. In particular, Kim *et al.* have proposed a Continuous Passive Motion machine that uses a 4-bar linkage to model specific motions of the knee joint in the sagittal plane [46]. In [47], movements of the knee in the sagittal plane is modeled using a linear actuated cam mechanism. However, given the unique nature of the knee motion for each individual, these exoskeletons necessitate offline adjustments for every individual, such that the device joint axes closely matches human knee joint axes. However, adjusting device joint axes to match the human axes is a tedious process that may take up an important portion of precious therapy duration.

More recently, knee exoskeletons that feature 3 active DoF in the sagittal plane have been introduced [48,49]. A planar mechanism with three revolute joints connected in series is proposed in [48], while in [49], a 3RRP pla-

13

nar parallel mechanism to allow for AP translations, while assisting flexion-extensions movements of the knee have been introduced [49]. The 3RRP mechanism acts as a mechanical summer, superimposing the torques of all three actuators to actuate rotation of the knee. Thanks to this feature, the resulting exoskeleton is back-driveable; hence, allows self-adjustment of the rotation axis of the exoskeleton during knee movements. Having 3 active DoF, this mechanism can also be utilized to impose desired AP translations to the knee.

Even though actuating all 3 DoF movements may be useful for certain therapies, commonly it is sufficient to only actuate flexion-extension of the knee, while being able to measure AP translations. Actuating only the rotational DoF, while keeping translational DoF under-actuated, helps the weight and complexity of the mechanism to be low. In [50], a 6 DoF knee exoskeleton with one active rotational DoF and 5 passive DoF have been proposed. Even though this device seems ideal from an ergonomic point of view, the design is relatively complex and heavy.

ASSISTON-KNEE is presented in [51], that can provide assistance for the flexion/extension of the knee joint, while simultaneously enabling and measuring its AP translations. In particular, ASSISTON-KNEE features 1 active rotational DoF controlled through a Bowden cable driven series elastic actuator, and 2 passive translational DoF in the sagittal plane. ASSISTON-KNEE is based on a planar parallel kinematic chain, commonly refereed to as Schmidt Coupling [52], and possesses a singularity free workspace that can cover the whole RoM of knee of a healthy human. ASSISTON-KNEE can passively enable AP translations of the knee joint to adjust its joint axes corresponding to knee rotation to provide an ideal match between human joint axes and the ex-

oskeleton axes. Thanks to this feature, ASSISTON-KNEE not only guarantees ergonomy and comfort throughout the therapy, but also extends the usable RoM for the knee joint. Adjustability feature also significantly shortens the setup time required to attach the patient to the exoskeleton. In addition to RoM measurements for the flexion/extension movements, ASSISTON-KNEE can measure AP translations, extending the type of diagnosis that can be administered using the knee exoskeletons. Furthermore, ASSISTON-KNEE possesses a light-weight and compact design with significantly reduced apparent inertia, thanks to its Bowden cable based transmission that allows remote location of the actuator and reduction unit. Due to its series elastic actuation, ASSISTON-KNEE enables high-fidelity force control and active backdriveability below its control bandwidth, while featuring passive elasticity for excitations above its control bandwidth, ensuring safety and robustness throughout the whole frequency spectrum.

An under-actuated Schmidt-coupling is selected as the underlying mechanism for implementation of ASSISTON-KNEE self-aligning knee exoskeleton, since this mechanism not only enables active control of the knee rotations, but also allows for passive translations of the exoskeleton axis throughout the knee motion. Furthermore, this mechanisms allows for the input rotation provided to be directly mapped to the knee rotation with exactly the same amount, independent of the translation of the rotation axis. Thanks to its parallel kinematic structure, the Schmidt coupling features higher rigidity and position accuracy, when compared to serial implementations of 3 DoF mechanisms. Schmidt coupling does not have kinematic singularities within its workspace[1] and can cover a large range of rotations, that is necessary for

---

[1]Singular configurations exist at the boundaries of ideal workspace; however, these singularities may simply be avoided by mechanically limiting the translational workspace

implementation of a knee exoskeleton with a range of motion exceeding 90°
during flexion and extension exercises.

2.3 Kinematic Analysis

A Schmidt coupling is a planar mechanism possessing 3 DoF: 2 DoF translations in plane and 1 DoF rotation about the axis perpendicular to this plane [53]. The mechanism consists of seven rigid bodies: the input ring I, the intermediate ring T and the output ring E, and two links A, B connecting I to T and two more links C, D connecting T to E. During a typical implementation, two redundant connecting links (one extra at each level) are also employed for extra rigidity, force distribution and better balancing. In Figure 2.2, the point O is fixed at the center of I, while point Z is fixed at the center of E. Points K, L, M and Q, R, S mark revolute joints at connection points of links A, B and C, D, respectively. The common out of the plane unit vector is denoted by $\vec{n}_3$, while basis vectors of each body are indicated in Figure 2.2. Symbol N depicts the Newtonian reference frame and is coincident with body I at instant $\theta_1 = 0$.

Let the center of output ring E with respect to the center of input ring I be expressed in the Newtonian frame as $x\,\vec{n}_1 + y\,\vec{n}_2$, while the orientation of I with respect to N be characterized by the angle θ_1. The, the output variables can be defined as $x = \vec{r}^{OZ} \cdot \vec{n}_1$, $y = \vec{r}^{OZ} \cdot \vec{n}_2$ and $\theta_2 = atan2(\vec{e}_2.\vec{n}_2, \vec{e}_1.\vec{n}_1)$.

Forward kinematics of the mechanism can be analytically derived both at configuration and motion levels. Forward kinematics is necessary to calculate the translations of the rotation axis of output ring E. A solution to the inverse kinematics of the mechanism is not necessitated by this application,

---

of the mechanism to be slightly smaller than its ideal limits.
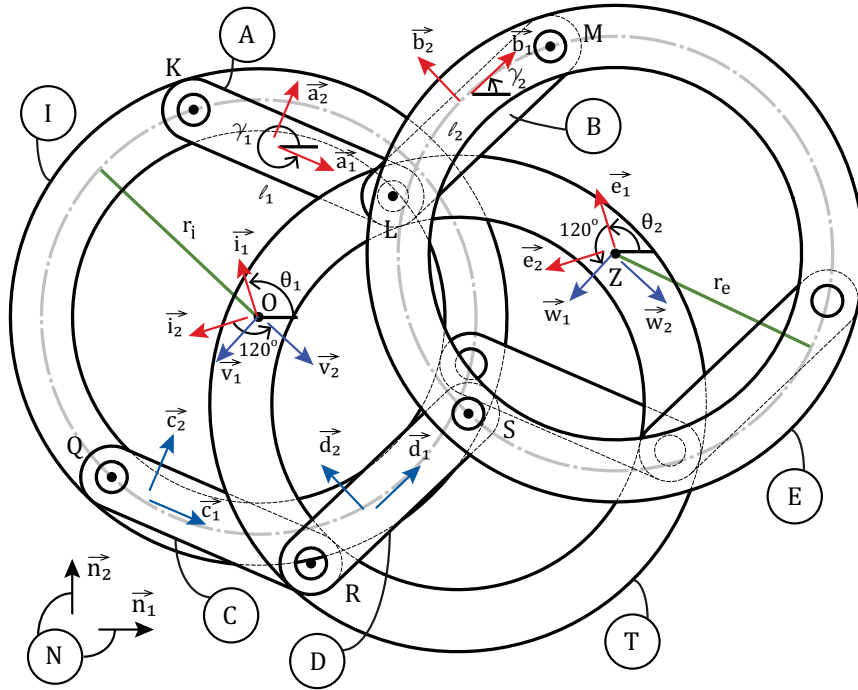
Figure 2.2: Schematic diagram of Schmidt coupling

since the joint space rotations are the measured quantities.

2.3.1 Configuration Level Forward Kinematics

In addition to rotation θ_1 of input link I with respect to N, the orientation of the connecting links A (and also C) and B (and also D) are measured with respect to bodies I and E and are indicated by the variables γ_1 and γ_2, respectively. For more compact representation, auxiliary reference frames V and W are introduced on the bodies I and E, respectively, by 120° simple rotations about $\vec{n}_3$.

Given the above definitions, the configuration level vector loop equations

of the mechanism can be expressed as

$$r_i \vec{i_1} + l_1 \vec{a_1} + l_2 \vec{b_1} - r_e \vec{e_1} - x \vec{n_1} - y \vec{n_2} = 0 \tag{1}$$

$$r_i \vec{v_1} + l_1 \vec{c_1} + l_2 \vec{d_1} - r_e \vec{w_1} - x \vec{n_1} - y \vec{n_2} = 0 \tag{2}$$

Expressing all vectors in the Newtonian reference frame N, following scalar constraint equations can be derived

$$r_i \cos \theta_1 + l_1 \cos \gamma_1 + l_2 \cos \gamma_2 - r_e \cos \theta_2 - x = 0 \tag{3}$$

$$r_i \sin \theta_1 + l_1 \sin \gamma_1 + l_2 \sin \gamma_2 - r_e \sin \theta_2 - y = 0 \tag{4}$$

$$r_i \cos(\theta_1 + \frac{\pi}{3}) + l_1 \cos \gamma_1 + l_2 \cos \gamma_2 - r_e \cos(\theta_2 + \frac{2\pi}{3}) - x = 0 \tag{5}$$

When $r = r_i = r_e$, Eqns. (3) and (5) imply that θ_2 should be equal to θ_1 or have a $\pm 120^o$ offset with respect to θ_1. Noting that all bodies considered in the analysis are symmetric with a $120°$ circular pattern, without loss of generality, one can use the solution

$$\theta_2 = \theta_1 \tag{6}$$

indicating that the amount of input and output rotations are the same for the mechanism. Imposing equal link lengths constraint to each connecting rod, that is $l = l_1 = l_2$, the translations of the output link can be calculated as

$$x = l \cos \gamma_1 + l \cos \gamma_2 \tag{7}$$

$$y = l \sin \gamma_1 + l \sin \gamma_2 \tag{8}$$

2.3.2 Motion Level Forward Kinematics

Taking the time derivatives of the vector loop equations (Eqns. (1) – (2)) with respect to N, and projecting the resulting vector equations onto the unit vectors $\vec{n_1}$ and $\vec{n_2}$, respectively, the variables $\dot{\theta}$, $\dot{x}$ and $\dot{y}$ characterizing the angular/translational velocities of the output link O can be derived as

$$
J = \begin{bmatrix} -lsin(\gamma_1) & -lsin(\gamma_2) & 0 \\ lcos(\gamma_1) & lcos(\gamma_2) & 0 \\ 0 & 0 & 1 \end{bmatrix} \tag{9}
$$

with $[\dot{x} \ \dot{y} \ \dot{\theta}_2]^T = J [\dot{\gamma}_1 \ \dot{\gamma}_2 \ \dot{\theta}_1]^T$, where J represents the kinematic Jacobian J of the Schmidt Coupling.

2.4 Design and Implementation of ASSISTON-KNEE

In this section details of design will be given. Singularity analysis of the proposed Schmidt coupling design and the solution to avoid these singularities are presented. Then simulations for structural analysis is realized in order to show that the design is safe against failure. Then, the actuation mechanism and implementation are explained in detail.

2.4.1 Singularity Analysis and Avoidance

Analyzing the kinematic Jacobian J, singularities of the Schmidt Coupling can be located to occur when $\gamma_1 = \gamma_2$ and $\gamma_1 = -\gamma_2$. Two configurations corresponding to samples of these singularities are depicted in Figure 2.3. At these singularities, forces acting on the output link cannot translate the mechanism; hence, the mechanism loses its self-adjustment feature. Luckily, since these singularities are located at the borders of the workspace of the

mechanism, they can be avoided by mechanically limiting the workspace of the device. In particular, perfect alignment of input and output discs can be avoided by introducing overlapping pins to the center of each disk, while fully extended configuration of connecting rods can be avoided by restricting the range of motion of the output disk (see Figure 2.5 for an implementation of such mechanical limits in ASSISTON-KNEE).
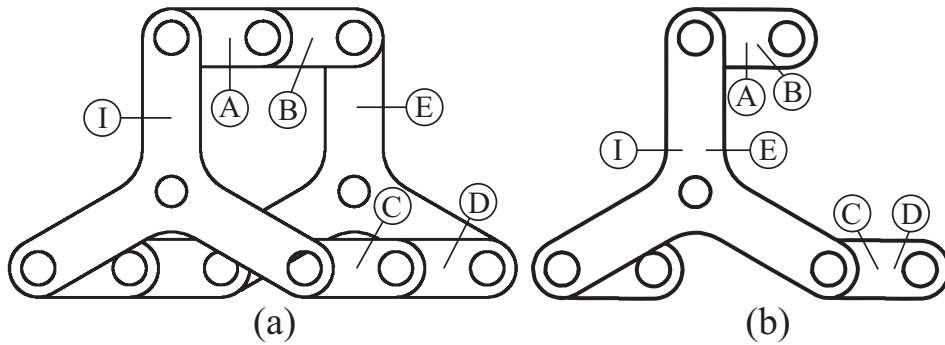
Figure 2.3: Kinematic singularities at (a) $\gamma_1 = \gamma_2$ and (b) $\gamma_1 = -\gamma_2$

2.4.2 Structural Analysis

Failure of all part in the design must be prevented. Thus, structural simulations of parts in terms of load carrying capacity are performed with finite element analysis tool embedded in SolidWorks Simulation CAD-embedded analysis (Cosmos). Although, it is possible to make components of a structural element safer by increasing its dimensions, such a choice results in a bulky design with high inertia. High inertias are not desired in exoskeleton designs, since it is harder to maintain safety and ergonomy of the user during physical interactions with the device. Along the lines of this trade-off, a better design that is somewhat over-safe but not too far away from the optimality is targeted. In particular, instead of solving an optimization
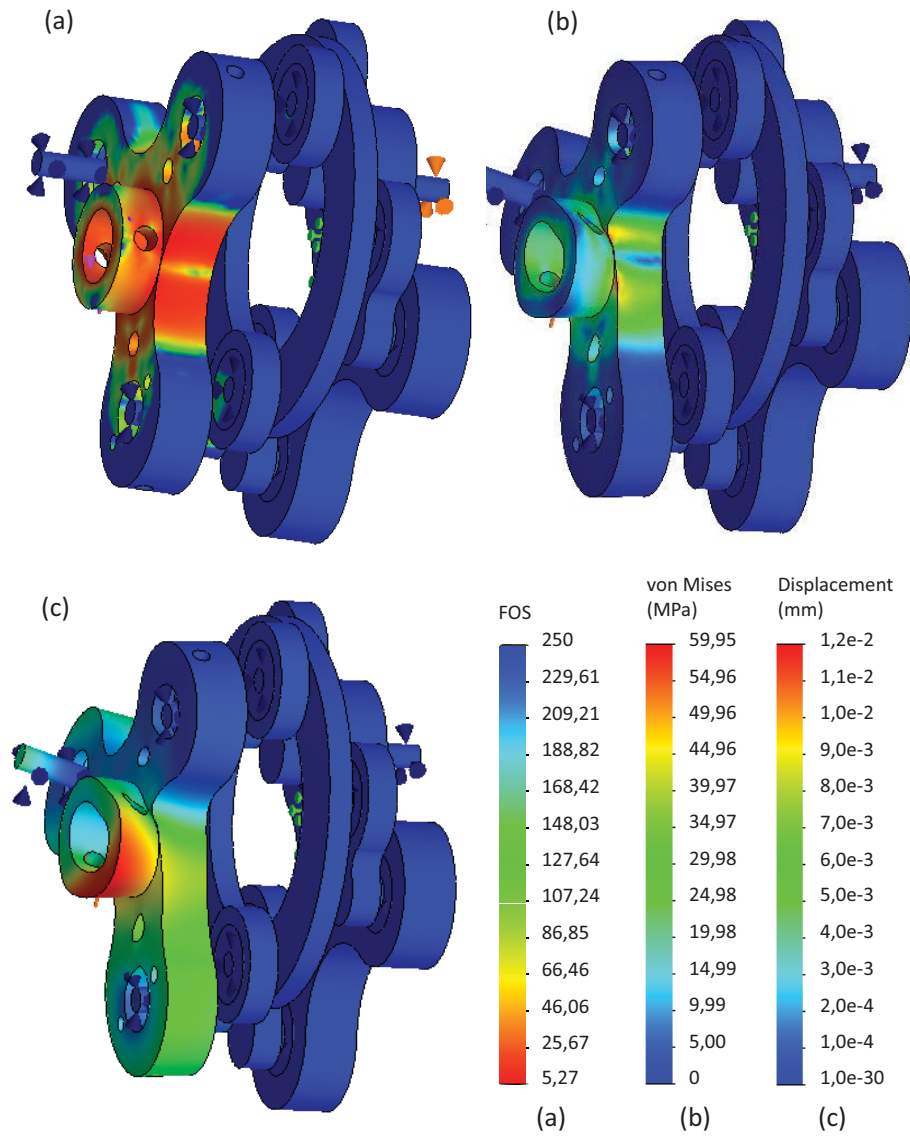
Figure 2.4: Structural analysis result of Schmidt coupling. (a)Factor of safety (b)von Mises Stress [MPa] (c)Displacement [mm]

problem, the design is performed iteratively, according to the results of the FEA simulations until an adequate design is decided upon.

Static performances of the most critical parts are analyzed using struc-

tural simulation. For ASSISTON-KNEE, Schmidt coupling is analyzed and sample results are presented in Figure 2.4. Schmidt coupling is constructed out of aluminum with a yield strength of 200 MPa. Besides, the bearings are considered in simulations and the assembly is considered to be free to move. A fixture is added to Body E of the coupling, while a torque input of 40 Nm is introduced to internal hollow face of Body I. Note that, the torque introduced is larger than the amount the device can apply (see Section 2.4.3). Gravity acting on the mechanism is neglected, since during use the device is fixed to human limb.

Finite element meshing is performed using 4 points Jacobian points with size of 1.9 mm for larger parts and 0.6 mm for critical and smaller parts. Corresponding results show that maximum stress that the coupling is subject to, is 60 MPa acting on Body I. Minimum observed safety factor is 5.3, resulting in a sufficiently safe design for rehabilitation use. Besides, maximum displacement observed is 12 micrometers. As the results show, the stress is mostly concentrated on Body I and the other bodies can have smaller stresses. However, due to other design constraints, such as symmetry of the mechanism and equal radius of discs, no further reduction of dimension is possible.

2.4.3 Bowden Cable-Driven Series Elastic Actuation and Implementation

Figure 2.5 presents a solid model of ASSISTON-KNEE which is implemented by designing a custom Schmidt Coupling to connect the thigh and shank of a patient, while the input disk of the Schmidt Coupling is actuated using a Bowden cable-driven series elastic actuator similar to the one used

22
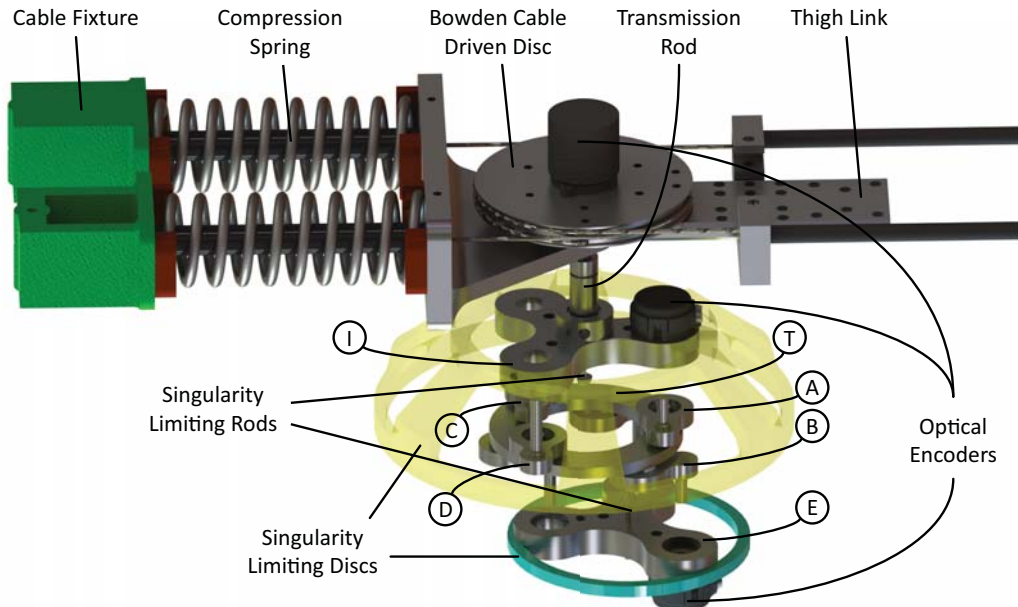
Figure 2.5:   Solid model of ASSISTON-KNEE

in [4]. Bowden cable enables the motor and gear reduction unit (see Figure 2.6) be placed away from the knee, enabling significant reduction on the weight of the knee exoskeleton. However, due to friction in Bowden cables and harmonic drive based reduction unit, the Bowden cable-driven disk is not backdriveable. To ensure high fidelity force control for assisting patients, while simultaneously reducing the output impedance of the system for safety, we have intentionally introduced compliant elements between the Bowden cable-driven disk and the input disk I. The input torque to the system is controlled by measuring the deflection between these two disks and applying Hook's law, given the effective torsional stiffness of the elastic coupling. In particular, the design alleviates the need for high-precision force sensors/actuators/power transmission elements and allows for precise control of the force exerted by Bowden cable-driven actuator through typical position control of the deflection of the compliant coupling element. Another

23
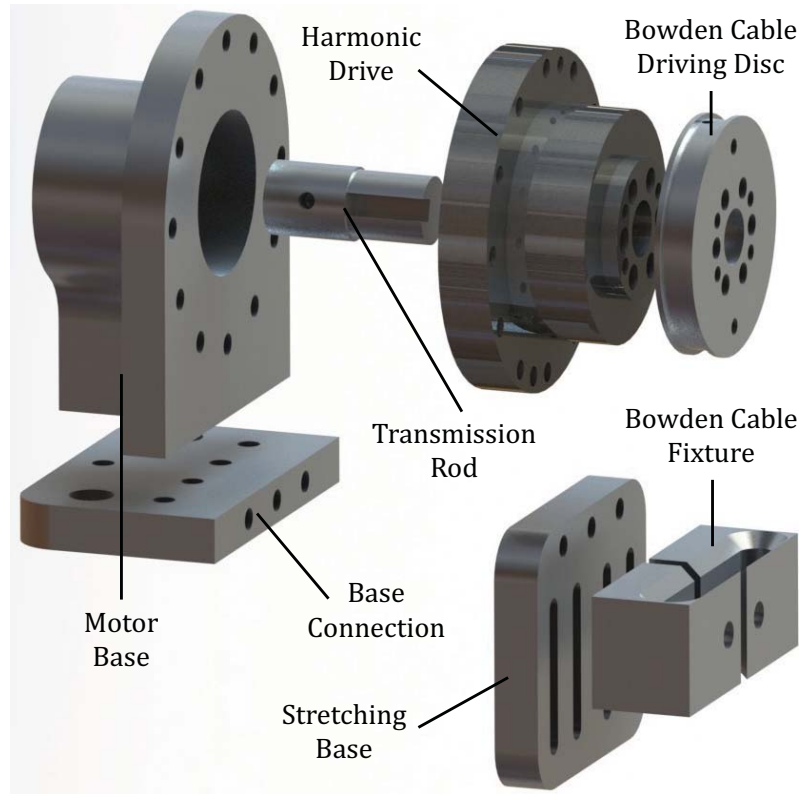
Figure 2.6: Solid model of the remote actuation unit

benefit due to series elastic actuation is the low output impedance of the system at the frequencies above the control bandwidth, avoiding hard impacts with environment [54]. Consequently, ASSISTON-KNEE can, not only ensure backdriveability though active control at frequencies below its control bandwidth, it also features a certain level of passive elasticity for excitations above its control bandwidth, ensuring safety and robustness throughout the whole frequency spectrum.

Control bandwidth of series elastic actuators are relatively low, due to the intentional introduction of the soft coupling element [55]. Force resolution of a series elastic actuator improves as coupling is made more compliant; however, increasing compliance decreases bandwidth of the control system,

trading off response time for force accuracy. Even though low bandwidth of series elastic actuator limits haptic rendering performance, this does not pose an important concern for rehabilitation robots, since high fidelity rendering is not an objective and the device bandwidth can still be kept significantly higher than that of patients to provide adequate levels of haptic assistance.

Figure 2.7 presents a functional prototype of ASSISTON-KNEE. A commercial knee brace is utilized to attach the exoskeleton to thigh and shank of the patient, while thigh and shank links are connected to each other through a custom built Schmidt Coupling on one side, and an unactuated RRR serial mechanism on the other. The RRR serial mechanism helps with structural integrate of the exoskeleton, while not restricting its movements in sagittal plane. Since ASSISTON-KNEE is self aligning, the exoskeleton can be worn in less than a minute, while it takes about 10 minutes to don and doff Roboknee [44].

The Schmidt Coupling is actuated by a series elastic actuator driven by Bowden cables. Bowden cable drive enables the actuator and harmonic drive to be remotely located, resulting in a light weight design with low apparent inertia. The part of the exoskeleton that is connected to human limbs weighs less than 1.4 kg. The remotely located actuation unit for the Bowden cables utilizes a 200W graphite brushed DC motor instrumented with an optical incremental encoder. A harmonic drive with a reduction ratio of 1:50 is used together with a Bowden cable disc ratio of 4:7 to deliver up to 35.43 Nm continuous torque to actuate flexion/extension rotations of the knee joint. The shields of Bowden cables are attached to a fixture that allows for easy stretching of the cables as presented in Figure 2.6 and 2.8. However, friction introduced to the system increases as the cables are bent with smaller radius.
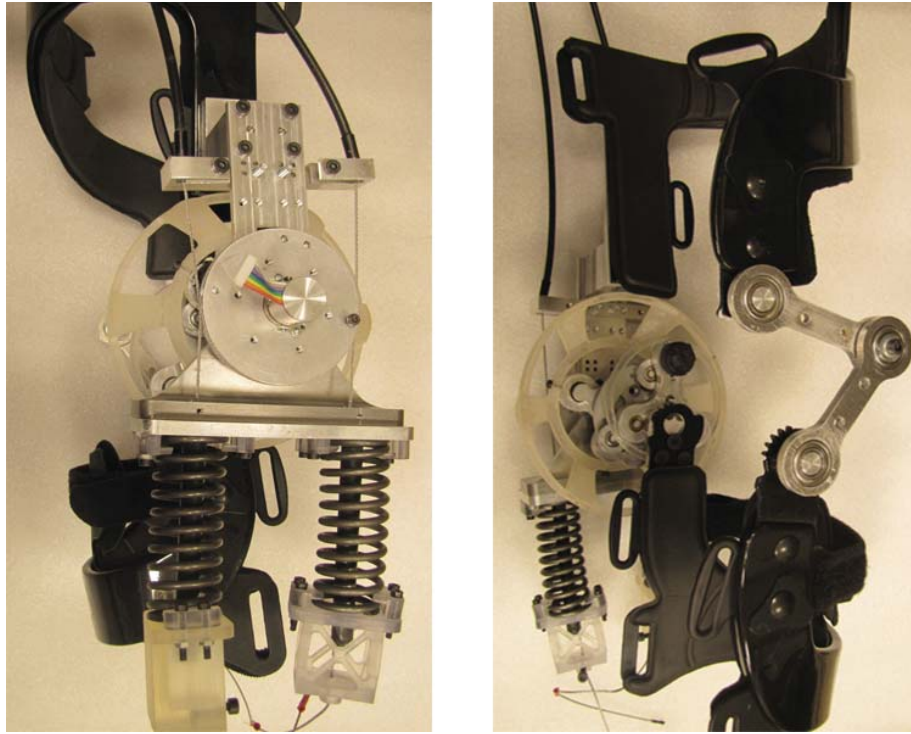
Figure 2.7: Prototype of Bowden cable-driven series elastic AssistOn-Knee

Incremental encoders are attached to the Schmidt coupling to measure relative rotations of the input disc I and the connection rods C and D. Thus, forward kinematics can easily be calculated.

2.5 Control and Experimental Characterization of AssistOn-Knee

Figure 2.9 shows the explicit force controller scheme that is used for controlling AssistOn-Knee. The desired torque is compared to actual measured torque in between actuator and exoskeleton where springs are placed thanks to the series elastic property of the device. A simple PD controller produces desired current on the motor where θ is the measured displacement of the device and q is displacement of the actuator.

Figure 2.8: ASSISTON-KNEE and its remote actuation unit

Moreover, table 2.1 presents the characterization results for ASSISTON-KNEE. Instantaneous peak and continuous end-effector torques are determined as 780 Nm and 35.5 Nm, respectively. The end-effector resolutions are calculated to be less than 0.05 for translations of the knee and 0.2° for rotations. Linear compression springs with spring rate of 10.3675 N/mm measured the torque with resolution of 0.0025 Nm and the device stiffness is 26 N/rad. The exoskeleton possesses a translational workspace that spans an area between two (singularity limiting) circles of radiuses 1 mm and 24 mm, while it is capable of performing up to 180° rotations about the perpendicular axis. Mechanical stops are utilized to limit the rotational range to match the requirements of the rehabilitation task. Specifications of the device is selected to be close to specifications of [56] which is a commercial

27
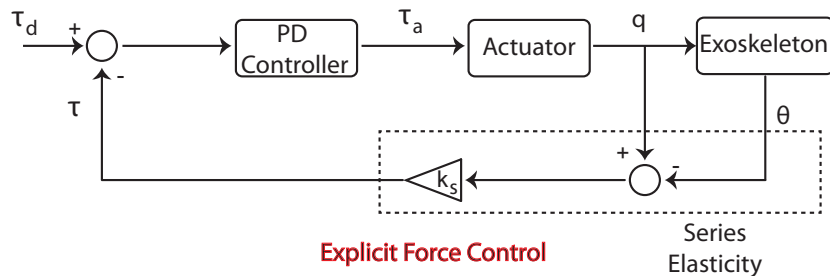
Figure 2.9: Controller design of ASSISTON-KNEE.

exoskeleton for knee rehabilitation.

2.6 Experimental Results

To test feasibility and useability of ASSISTON-KNEE to assist knee movements, we have tested flexion/extension movements of healthy volunteers under closed-loop position of the robot. In particular, rotational flexion/extension movement is imposed to the subject, while AP translations in the sagittal plane are measured. A 2.5 Hz sinusoidal reference trajectory with 60° magnitude is imposed under a simple PD controller to the input of the Schmidt Coupling to carry out the knee flexion/extension, while volunteers are attached to ASSISTON-KNEE. Figure 2.10 presents AP translations of the

Table 2.1: Characterization of ASSISTON-KNEE

Criteria	X	Y	Z
Peak Torque	Not actuated	Not actuated	780 [Nm]
Cont. Torque	Not actuated	Not actuated	35.5 [Nm]
Max. Speed	Not actuated	Not actuated	65 [rpm]
Min. Resolvable Torque	Not actuated	Not actuated	0.0025 [Nm]
Device Stiffness	Not actuated	Not actuated	26 [Nm/rad]
Resolution	0.047 [mm]	0.047 [mm]	0.18 [°]
Workspace	-24 − 24 [mm]	-24 − 24 [mm]	-10° − 170°
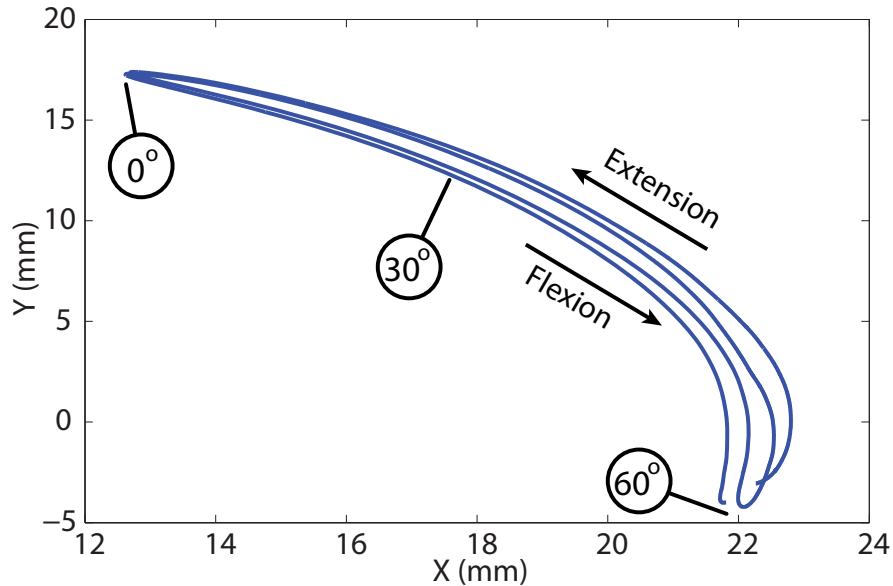
Figure 2.10: Knee joint center displacement

knee measured during this sample trial. Here, encirclements refer to flexion/extension angle of the knee. One can observe from Figure 2.10 that, as expected, knee follows a distinct closed loop trajectory during flexion and extension. ASSISTON-KNEE is capable of measuring AP translations, which may be useful for diagnostic purposes.

Besides, figure 2.11 presents torque tracking performance under explicit force control of ASSISTON-KNEE worn by a volunteer. The data is collected during a sample trial under a sinusoidal torque reference. As can be observed from this sample trial, the torque tracking performance is quite satisfactory for rehabilitation exercises. Small values of torque ripples (with rms value of 74.3 Nmm) can be observed because of stick-slip friction due Bowden cables and the harmonic drive and because of quantization noise in the encoders. Luckily, actuation torques are mechanically low pass filtered by the spring elements before being applied to patients. Furthermore, effort of the user is compared in figure 2.12 for flexion and extension of knee with and without

29
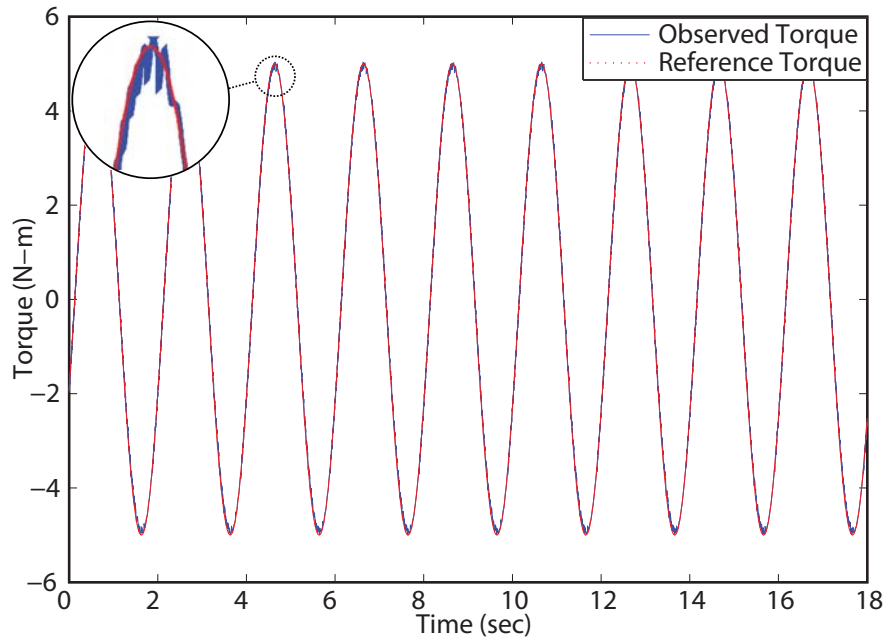
Figure 2.11: Torque tracking performance of AssistOn-Knee under a sinusoidal torque reference

AssistOn-Knee where the reference of the controller is the data taken from the results of experiment without AssistOn-Knee. Due to the nature of the task, AssistOn-Knee is not effective on flexion assistance, but it remarkably decreases the effort for extension. Quadriceps femoris and medial hamstring muscle groups are selected to get EMG signals from.
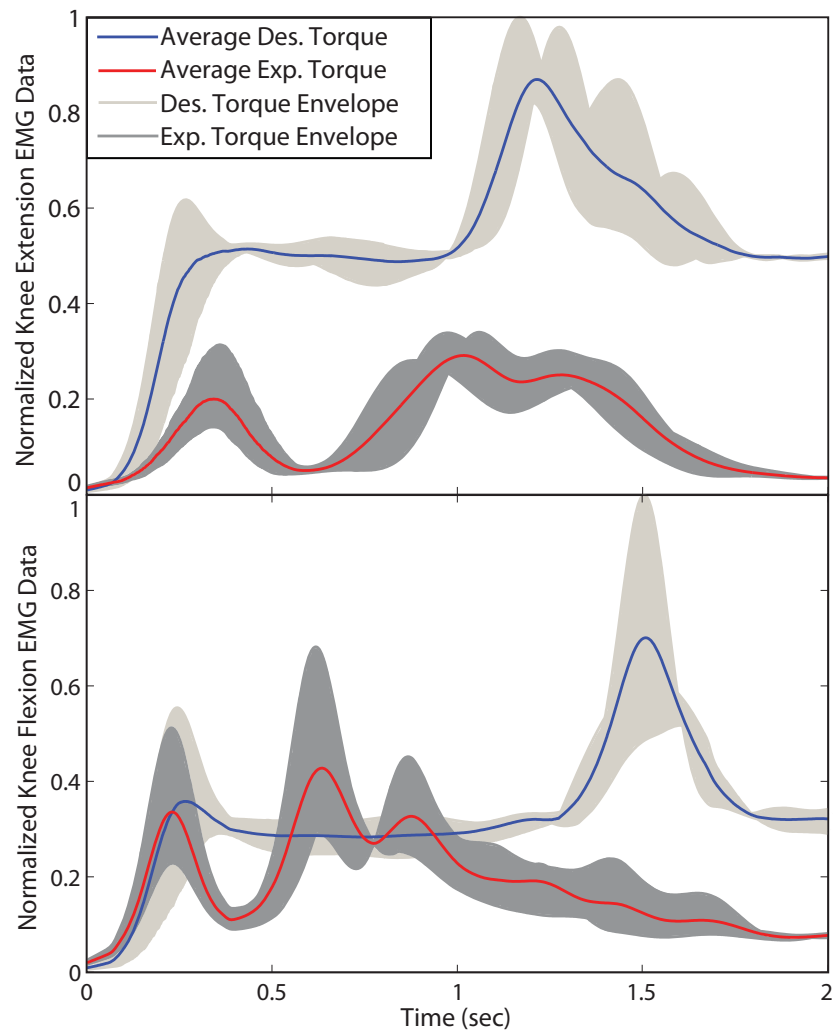
Figure 2.12: Normalized EMG signal levels for knee flexion and extension muscles during a standing up task with and without assistance

Chapter III

3   ASSISTON-ANKLE

This chapter explains the motivation, kinematics and design of ankle exoskeleton ASSISTON-ANKLE along with kinematics of human ankle joint.

3.1   Kinematics of Human Ankle
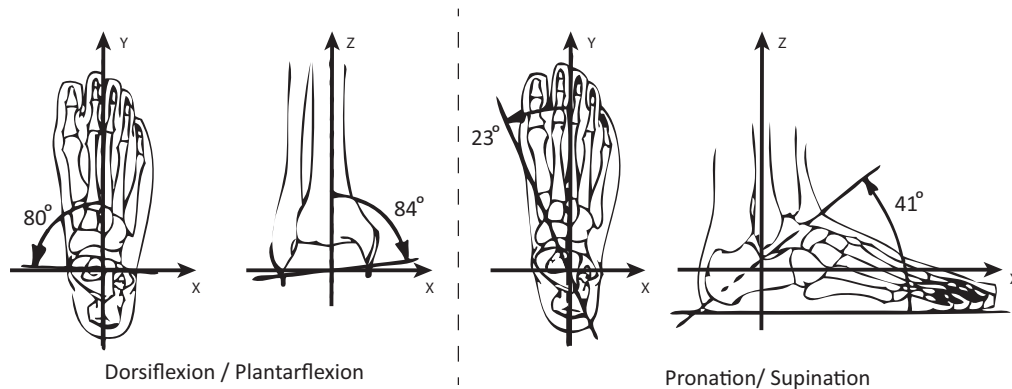
Figure 3.1: Kinematics of the human ankle

Dominant movement at ankle joints are given as plantarflexion/dorsiflexion, abduction/adduction and inversion/eversion [57]. However, the kinematics of ankle joint is complicated. Modeling ankle joint is realized by spherical joint models which basically makes use of 3 intersecting axes at a single point [58,59]. On the other hand, [60] whose model is verified and made use of in biomechanics literature, claims that the motion at the foot is coupled and

Table 3.1: Requirements of the Human Ankle Joint

Joint	Joint Torque Limits	Joint RoM
Dorsiflexion\	40.7–97.6 Nm	20°
Plantarflexion	20.3–36.6 Nm	40°
Inversion\	max 48 Nm	35°
Eversion	max 34 Nm	25°

a 2-revolute-joint (RR) serial kinematic chain is sufficient for modeling ankle joint. This chain is composed of an upper ankle joint which supports rotational dorsiflexion/plantarflexion motion and a subtalar joint that supports the rotational supination/pronation motion which is a complicated motion and is composed of abduction/adduction and inversion/eversion motions. Figure 3.1 indicates the axes of these motions, based on [61]). However, due to variety of sizes, shape and orientations of foot articulation, ligaments and muscles, the motion at the ankle is unique for every individual. Table 3.1 shows the RoM and force/torque-bearing capability requirements of ankle joint based on the data given in [62]. Whereas, statistical dimension data of foot and ankle is given in Table 3.2 depending on [63]. Furthermore, when the human leg is under no load, internal/external rotation of the human knee is observed and it affects the configuration of the ankle joint. Thus, another revolute joint can be introduced to model kinematics of the human ankle with respect to human knee. The overall kinematic chain is a 3-revolute-joint (RRR) series kinematic chain.

3.2 ASSISTON-ANKLE

Ergonomy in an exoskeleton is one of the most crucial feature that enables effective use of that exoskeleton for rehabilitation therapies. However, apart

Table 3.2: Foot Measurement Data

Body part	5th percentile	95th percentile
Ankle circumference	200 mm	245 mm
Ball of foot circumference	229 mm	275 mm
Bimalleolar breadth	67 mm	81 mm
Calf circumference	336 mm	432 mm
Calf height	316 mm	405 mm
Foot breadth	92 mm	111 mm
Foot length	249 mm	298 mm
Heel-ankle circumference	313 mm	375 mm
Heel breadth	62 mm	82 mm
Kneecap (patella) height	468 mm	569 mm
Lateral malleolus height	58 mm	78 mm
Medial malleolus height	76 mm	97 mm

from ergonomy, parallel mechanism are preferable to serial mechanisms due to their better satisfying force feedback applications with the help of compact designs with high stiffness, low effective inertia and high position/force bandwidth. Also precision of the parallel mechanisms are higher since superimposition of position errors at joints is not realized.

The devices which has series kinematics chains for human ankle, are few in number. Agrawal *et al.* introduced an orthosis in [64] that enables both two rotations of human ankle about their complex axes. However, this device needs offline adjustment since the axes are fixed throughout the therapy and the orientation of these axes are unique for every individual. Besides, most of the devices make use of parallel manipulators. End-effector type devices such as Rutgers Ankle [65], with high DoFs are firstly introduced. Case studies of different versions of this device is further studied in [66–68]. Later on, the devices with sufficient DoFs are introduced such as [58] which is used for robotic rehabilitation of sprained ankle. However, these type

of devices correspond with the human only at the end-effector and allow compensatory movements. On the other hand exoskeleton type robots allows control of joints individually since they correspond with human joints and allows no/little compensatory movements. Thus, they are capable of better application of different types of therapies such as RoM/strenghtning. Yet, devices such as [69] or [70] is designed to assist only specified movements of ankle which is plantarflexion/dorsiflexion. Whereas, devices like Anklebot, models ankle by approximating its movements to 2 DoF [71]. Furthermore, in [72], reconfigurability of devices is proposed to promote different types of rehabilitation exercises.

A rehabilitation device should cover the whole RoM of human at the specific joint which the device is designed for. For the case the ankle joint, an underactuated parallel 3U$\underline{\text{P}}$S manipulator can cover the whole RoM while it also can adopt for different dimensions of the foot. Although it has 6 DoF, only 3 actuators are used to control prismatic joints and this underactuated device is meaningless by itself. But, human foot becomes the part of the kinematics when it is worn by the user and the device has 3 DoF that the user exerts. Thus, ergonomy of the device is maintained.

The 3U$\underline{\text{P}}$S-RRR is useful for RoM/strengthing exercises since human ankle is set as a part of the kinematics. Yet, for balance/proprioception exercises this manipulator is not preferable since the torque/force transferred to the human ankle cannot be supported. A parallel R-3R$\underline{\text{P}}$S manipulator on the other hand, can support human weight, accommodate the torques transferred to the ankle and cover acceptable part of human ankle workspace. This manipulator has 3 DoF and actuation is realized on the prismatic joints. Unlike the 3U$\underline{\text{P}}$S manipulator, human foot kinematics becomes redundant when

35

the device is worn by the user and the kinematics of the manipulator is dominating the system kinematics. Besides, to comply with the internal/external rotation of the human foot, the base of both manipulators is actuated which allows effective workspace of the device with 3R$\underline{\text{P}}$S manipulator to cover natural movements of human. Yet, this passive rotation is locked in the 3U$\underline{\text{P}}$S manipulator since it is assisted.

On the other hand, AssistOn-Ankle has the advantages of both 3R$\underline{\text{P}}$S and 3U$\underline{\text{P}}$S manipulators with the help of a reconfigurable mechanism. Besides, these two manipulators are the most suitable to serve as an exoskeleton under force feedback since they are compact and avoid collisions with human foot while promoting its motion. Although there are advances recently in type synthesis of parallel mechanisms [73–75], analysis of some most basic types are not realized in detail [76]. However, kinematic and singularity analysis of both 3R$\underline{\text{P}}$S and 3U$\underline{\text{P}}$S manipulators takes place in the literature.

(a)R-3-R$\underline{\text{P}}$S   (b) 3-U$\underline{\text{P}}$S-RRR
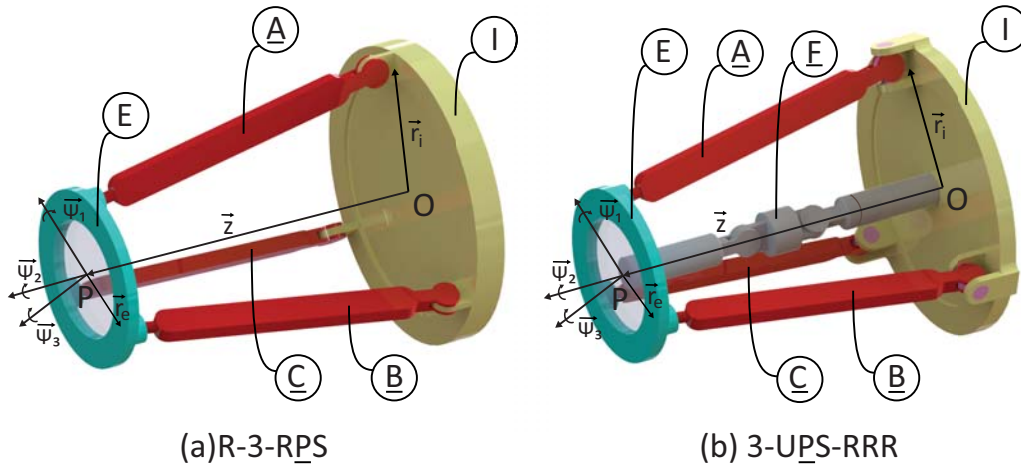
Figure 3.2: R-3R$\underline{\text{P}}$S and 3U$\underline{\text{P}}$S-RRR mechanisms

3.3 Kinematic Analysis

Lee *et al.* introduced the 3R$\underline{P}$S parallel manipulator firstly [77]. Then, more advanced analysis of this manipulator is made in [78]. Using this mechanism as an exoskeleton is firstly realized by Gupta *et al.* [79] with a wrist exoskeleton and then the idea is adopted to a wrist rehabilitation device in [80]. Furthermore, in [81] and [82], design optimization of the manipulator for force feedback applications is discussed. Basically, the mechanism is composed of 5 bodies; a base platform (I), a moving platform (E) and 3 extensible links (A,B,C). Extensible links are connecting the base platform and the moving platform. The connections of links and base platform are revolute joints, whereas they are spherical joints in between links and moving platform.

Although the internal/external rotation of the foot is maintained with a passive revolute joint that rotates the base platform with respect to the Newtonian reference frame, kinematic analysis is derived only for the 3R$\underline{P}$S mechanism which is selected as symmetric for the design of ASSISTON-ANKLE. The revolute joints are placed on a circle with radius r_i using a 120° spaced pattern. The same circular pattern is used for placement of spherical joints on the moving platform with radius r_e.

The 3R$\underline{P}$S manipulator has 3 DoF which are the distance between the moving platform center and base platform center, namely z and two rotations, Ψ_1 and Ψ_2, of the moving platform with respect to the Newtonian reference frame. The actuation is imposed by controlling the length of the extensible links. The motion in the transverse plane is limited by the spherical joint limits and extensible link lengths and for the joint angles less than $\pi/2$ no singularity is observed [77].

On the other hand, the 3U<u>P</u>S-RRR manipulator is composed of 6 bodies; a base platform (I), a moving platform (E) and 3 extensible links (A,B,C) similar with the 3R<u>P</u>S manipulator and an additional center link (F). Besides, unlike the 3R<u>P</u>S mechanism, the joints that are connecting base platform and extensible links are universal. Since the end-effector, which is the moving platform, is tightly connected to human foot, the center link is realized with human ankle that can enable 3 series revolute joint mechanism (RRR). Thus, human ankle is part of the kinematics with this mechanism[2]. The design of the 3U<u>P</u>S mechanism is symmetrical in the same manner of 3R<u>P</u>S mechanism with the same dimensions of bodies.

The 3U<u>P</u>S-RRR manipulator has 3 DoF which are aforementioned upper ankle joint, subtalar joint (see 3.1 subsection) and knee internal/external rotation that imposes a coupled motion of the moving platform with respect to Newtonian reference frame. The actuation is realized by controlling the length of the extensible links. Translational motions in transverse plane for this mechanism, is not allowed.

By decoupling the parallel 3U<u>P</u>S manipulator and spatial RRR mechanism and analyze them separately, forward and inverse kinematics of 3U<u>P</u>S manipulator can be derived. By denoting x, y, z as the translations and ψ_1, ψ_2, ψ_3 as the rotations of the moving platform, q_1 and q_2 as the rotation of the ankle about its joint axes with respect to Newtonian reference frame, s_1, s_2, s_3 as the length of the extensible links and ϕ_1, ϕ_2, ϕ_3 as the rotations of the extensible links about their axes which are the revolute joint axes used in 3R<u>P</u>S mechanism, motion level forward kinematics of 3U<u>P</u>S manipulator

---

[2]Note that since human ankle makes redundant constraints to come up for 3R<u>P</u>S mechanism unlike for 3U<u>P</u>S, it is unnecessary to consider it as a part of the kinematics of 3R<u>P</u>S manipulator

can be derived using the analytic Jacobian as:

$$[\dot{x} \ \dot{y} \ \dot{z} \ \dot{\psi}_1 \ \dot{\psi}_2 \ \dot{\psi}_3]^T = J_{3U\underline{P}S} \ [\dot{s}_1 \ \dot{s}_2 \ \dot{s}_3 \ \dot{\phi}_1 \ \dot{\phi}_2 \ \dot{\phi}_3]^T \qquad (10)$$

Whereas rotation of the human ankle can be found using the inverse Jacobian of the spatial RRR mechanism as:

$$[\dot{q}_1 \ \dot{q}_2 \ \dot{q}_3]^T = J_{RRR}^{-1} \ [\dot{x} \ \dot{y} \ \dot{z} \ \dot{\psi}_1 \ \dot{\psi}_2 \ \dot{\psi}_3]^T. \qquad (11)$$

Using the motion level forward kinematics of 3U$\underline{P}$S mechanism and inverse kinematics of spatial RRR mechanism, one can easily get the motion level forward kinematics of the 3U$\underline{P}$S-RRR mechanism as:

$$[\dot{q}_1 \ \dot{q}_2 \ \dot{q}_3]^T = J_{RRR}^{-1} \ J_{3U\underline{P}S} \ [\dot{s}_1 \ \dot{s}_2 \ \dot{s}_3 \ \dot{\phi}_1 \ \dot{\phi}_2 \ \dot{\phi}_3]^T. \qquad (12)$$

After deriving the inverse kinematics of the 3U$\underline{P}$S-RRR manipulator likewise, kinematics maps the measured data to actual rotation of the ankle joint or the joint torques at the ankle. Thus, it is helpful for RoM and maximum joint torque calculation.

3.3.1 Kinematics of the 3U$\underline{P}$S Mechanism

The 3U$\underline{P}$S manipulator has 6 DoF and for accurate use of this device, both configuration and motion level kinematics are required. To derive configuration level kinematics of the 3U$\underline{P}$S manipulator, closed vector loop equations

with 9 unknowns, are written as:

$$\vec{r}^{OI_A} + \vec{r}^{I_A E_A} + \vec{r}^{E_A P} + \vec{r}^{PO} = \vec{0} \tag{13}$$

$$\vec{r}^{OI_B} + \vec{r}^{I_B E_B} + \vec{r}^{E_B P} + \vec{r}^{PO} = \vec{0} \tag{14}$$

$$\vec{r}^{OI_C} + \vec{r}^{I_C E_C} + \vec{r}^{E_C P} + \vec{r}^{PO} = \vec{0} \tag{15}$$

The point O is fixed in body I and the point P is fixed in body E as shown in 3.2. Moreover, the bodies that are used to derive kinematics are shown in the figure. The inverse kinematic problem has trivial solution, whereas the forward kinematic problem needs extra measurement from the system since the mechanism has 6 DoF but, only three of them are measured along with the actuators for feedback control. To overcome this issue, 3 more state of the system should be known. So, additional rotary encoders are used to sense rotations, ϕ_1, ϕ_2 and ϕ_3. Then, by using numerical control techniques over nonlinear closed loop equations, end-effector configuration of the underactuated mechanism can be obtained uniquely. By taking derivative of the closed loop equations with respect to time, motion level kinematics of the 3U$\underline{\text{P}}$S manipulator can be derived.

$$^A\vec{v}^{E_A} + {}^I\vec{w}^A \times \vec{r}^{I_A E_A} + {}^I\vec{w}^E \times \vec{r}^{E_A P} - {}^I\vec{v}^P = \vec{0} \tag{16}$$

$$^B\vec{v}^{E_B} + {}^I\vec{w}^B \times \vec{r}^{I_B E_B} + {}^I\vec{w}^E \times \vec{r}^{E_B P} - {}^I\vec{v}^P = \vec{0} \tag{17}$$

$$^C\vec{v}^{E_C} + {}^I\vec{w}^C \times \vec{r}^{I_C E_C} + {}^I\vec{w}^E \times \vec{r}^{E_C P} - {}^I\vec{v}^P = \vec{0} \tag{18}$$

$\vec{v}$ and $\vec{w}$ represent relative velocities and angular velocities, respectively. Analytic Jacobian can be derived by solving the linear equations 16 for the time rate of change of end-effector coordinates using time rate of change of

measured coordinates data where the solution is unique. Besides, the transpose of the analytic Jacobian is used to map the end-effector forces to joint torques.

Consequently, the Analytic jacobian is the tool that uses mathematical mappings to determine the joint force/torques and configuration of the end-effector using the sensory data.

3.3.2 Kinematics of the 3R$\underline{\text{P}}$S Mechanism

The closed loop equations, 13 and the same notation with 3U$\underline{\text{P}}$S can also be used to derive kinematic analysis of 3R$\underline{\text{P}}$S manipulator since the structure of the mechanisms are very similar. Thus, the Analytic Jacobian that maps the joint force/torques and configuration of the end-effector to the sensory data is obtained by solving the time derivative of the closed loop equations, similarly.

Unlike the 3U$\underline{\text{P}}$S manipulator, there are no need for extra sensory data in 3R$\underline{\text{P}}$S manipulator. Besides, the human ankle kinematics is redundant when the foot is attached to the manipulator and the kinematics of the manipulator is dominant.

3.4 Design & Implementation of AssistOn-Ankle

The design of the exoskeleton is realized using the description of the 3U$\underline{\text{P}}$S and 3R$\underline{\text{P}}$S manipulators. The manipulators both has bodies; moving platform, base platform and 3 extensible links. The joints that connect the extensible links to the moving platform is spherical, whereas the ones that connects the links to base platform is revolute in 3R$\underline{\text{P}}$S manipulator and spherical in 3U$\underline{\text{P}}$S manipulator. And both mechanisms are desired since

they are effective on different types of rehabilitation therapies as mentioned in 3.2 subsection. In order to have both manipulators in a single exoskeleton, an interchangeable passive joint module with 2 revolute joint in series is designed as suggested in [83]. The axes of this joint coincides at a single point and in 3UPS manipulator, it works as a regular spherical joint while in 3RPS manipulator becomes a simple revolute joint by locking one of the revolute joints. Designing interchangeable joint that makes the device reconfigurable, allows the ankle exoskeleton to have 2 modes of operation, namely 3RPS mode and 3UPS mode and thus, different number of DoFs. Cost efficiently rearrangement of system components in the design is maintained with the help of reconfigurability [84, 85].

3UPS Mode   3RPS Mode
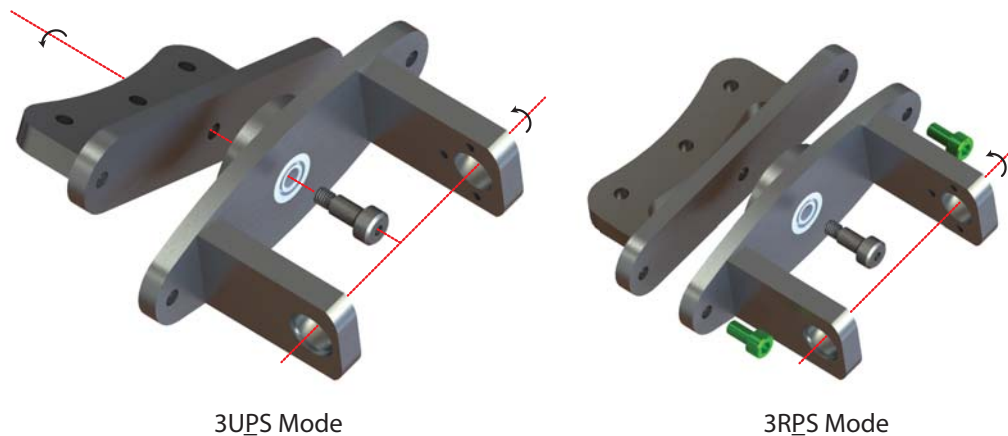
Figure 3.3: Interchangeable joint as universal and revolute joint

Use of interchangeable joints or actuators is not frequent for robotic rehabilitation purposes even though many of the existing passive medical devices make us of interchangeable components for various types of therapy and use of these interchangeable components is essential in rehabilitation robots since they promote ergonomy and hygiene. Some devices that exceptionally use

interchangeable parts are the ankle device [62] and a modular whole-arm device [86] where modular design allows the device to be used as a whole-arm robot that makes use of integrated modules or with a stand-alone mode that gives therapy for particular disorders, exemplarily. Furthermore, reconfigurability by changing or repositioning components is desired in [62] in order to allow a ROM/strengthing therapy device to work as a balance/proprioception therapy device [72].

In the sense that reconfiguration is used to change the kinematics of the device so that it is effectively used for both RoM/strengthing and balance/proprioception exercises, ASSISTON-ANKLE is similar to [72]. Interchangeable joint design is realized with the help of preventing one rotation by bolts as shown in 3.3. For the case where there is no bolt interchangeable behaves as a revolute joint and ASSISTON-ANKLE works in 3U$\underline{\text{P}}$S mode, whereas use of at least one bolt makes the joint universal and enables 3R$\underline{\text{P}}$S mode. Furthermore, in a similar manner, locking the passive rotation of R-3R$\underline{\text{P}}$S manipulator that allows knee internal/external rotation, assistance for this motion in 3U$\underline{\text{P}}$S-RRR manipulator is maintained.

Besides, dimensions at home configuration is selected for vertical distance between base and moving platforms as 375 mm, radius of the base platform as 165 mm and the radius of the moving platform as 84 mm, according to [87] where optimal design of reconfigurable ankle exoskeleton that exerts both 3R$\underline{\text{P}}$S and 3U$\underline{\text{P}}$S modes is studied. The workspace for both mechanisms are maintained with 100 mm of actuator range and for measured joint position of 3U$\underline{\text{P}}$S manipulator, allowable range between $-30°$ and $-7°$. Moreover, the symmetric design of the device enables it to be used for both foot. However, by connecting it to ASSISTON-KNEE, use of ASSISTON-ANKLE is limited to

(a) 3R<u>P</u>S   (b) 3U<u>P</u>S
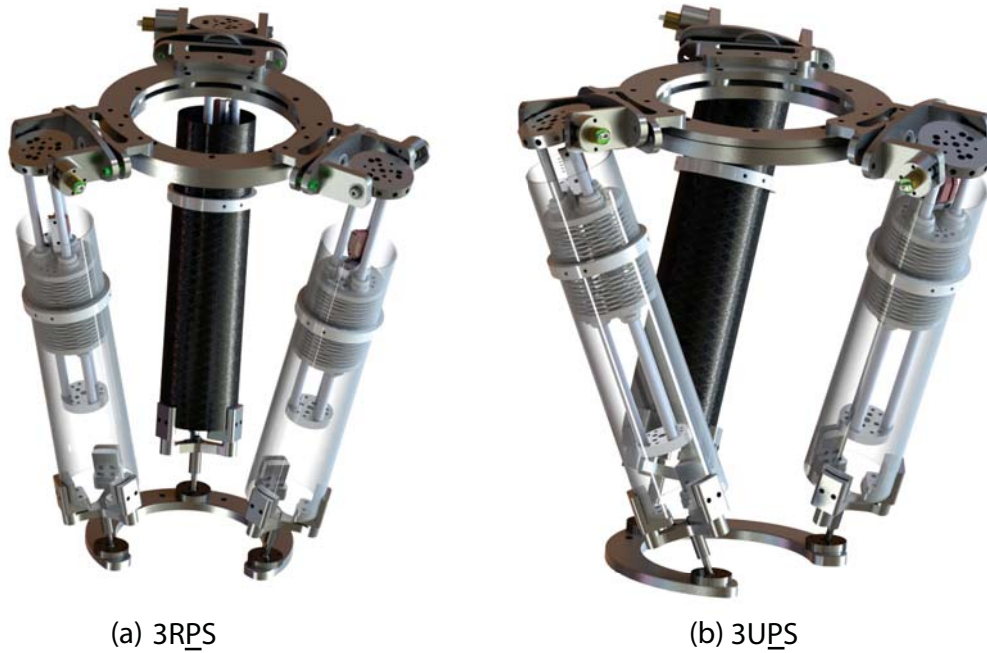
Figure 3.4: ASSISTON-ANKLE in 3U<u>P</u>S and 3R<u>P</u>S mode.

one leg. The final design of the reconfigurable ankle rehabilitation exoskeleton robot, ASSISTON-ANKLE is given in Figure 3.4 in both 3R<u>P</u>S and 3U<u>P</u>S mode.

3.4.1 Structural Analysis

Structural simulations of the end-effector of ASSISTON-ANKLE is performed with finite element analysis tool embedded in SolidWorks Simulation CAD-embedded analysis (Cosmos). Corresponding results are given in Figure 3.5. The materials used in the design is made of aluminum with yield strength of 200 MPa and carbon fiber roll wrapped twill tube with ultimate tensile strength of 4825 MPa. The end-effector has a rigid structure and analyzed as a single part. The fixture is added to the end-effector tip which is the

spherical joint head. Whereas, the input of 100 N is introduced to the central disc of the series elastic actuator to create tension on the end-effector. Note, that the introduced torque value is much larger than the device can apply (see Section 2.4.3). Gravity of the mechanism is neglected since the device is fixed to human limbs and carried by them.

Meshing is done using 4 points Jacobian points with size of 1.6 mm for larger parts and 0.6 mm for smaller parts. Corresponding results shows that maximum stress that the coupling is composed to, is only 6,2 MPa and concentrated on the spherical joint and the body where spherical joint is connected. Minimum observed safety factor is 35,6 which is more than sufficient for use of the device undoubtedly. Besides, maximum displacement is 6 micrometers.

Apart from the end-effector, the highest load is on the shoulder bolt of the interchangeable joint where the 3U$\underline{\text{P}}$S mode is active. The series elastic actuator is connected to the base platform only with this bolt. So, in simulations, 100 N force is applied on this bolt from its shoulder where it is fixed from the teeth rigidly and from the lower face of the bolt head with slider fixture. The corresponding results are shown in Figure 3.6. Meshing is realized similarly and the results show that maximum load is 43,5 MPa and concentrated on the edges of the shoulder. Minimum factor of safety of the bolt is 5 which is sufficient for the design and the maximum displacement is 1 micrometer which is such a small value.

3.4.2 Bowden Cable-Driven Series Elastic Actuation

The idea of Bowden cable-driven series elastic actuation is the same with the mentioned idea in Chapter II, Section 2.4.3. AssistOn-Ankle also
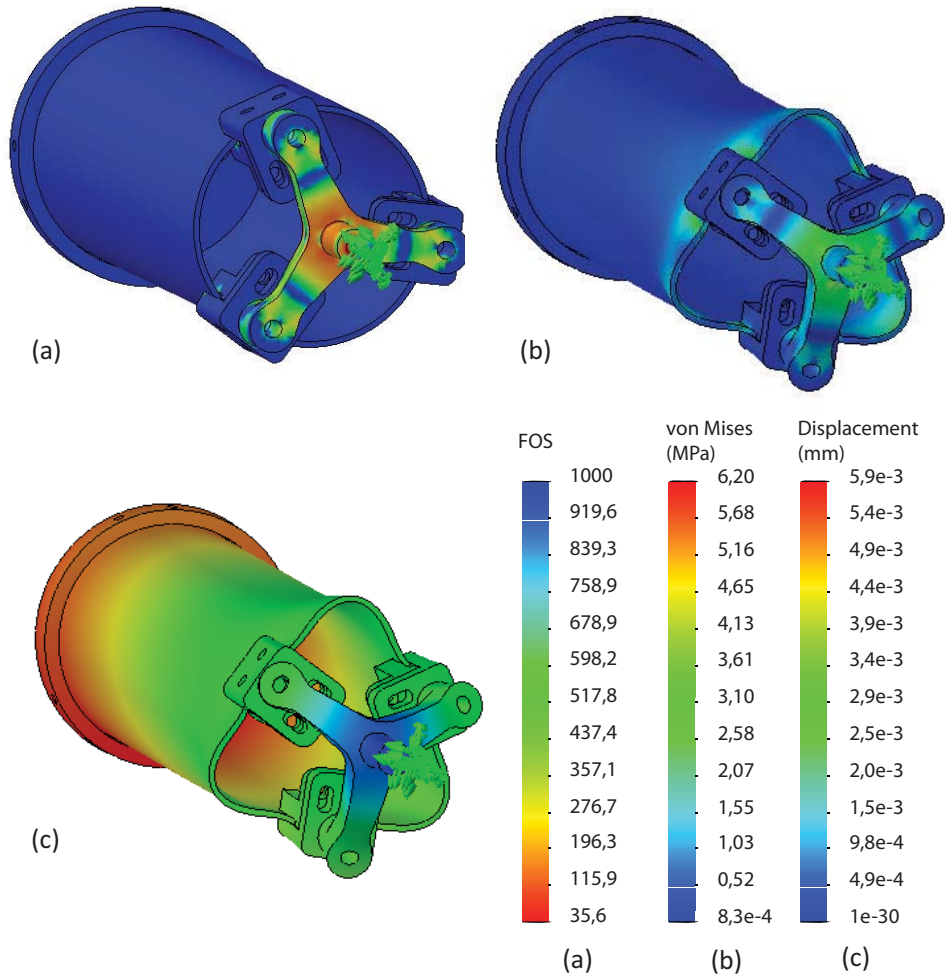
Figure 3.5: Structural analysis result of ASSISTON-ANKLE end-effector. (a)Factor of safety (b)von Mises Stress [MPa] (c)Displacement [mm]

benefits the advantages of Bowden cable-driven series elastic actuation of ASSISTON-KNEE. Since the direct drive mechanisms introduce additional weight to the system, ASSISTON-ANKLE makes use of cable-driven actuation and to ensure safety and robust controllability series elastic actuator design is realized. Furthermore, remote actuation unit of ASSISTON-ANKLE differs from the one used in ASSISTON-KNEE with the tensioning mechanism and
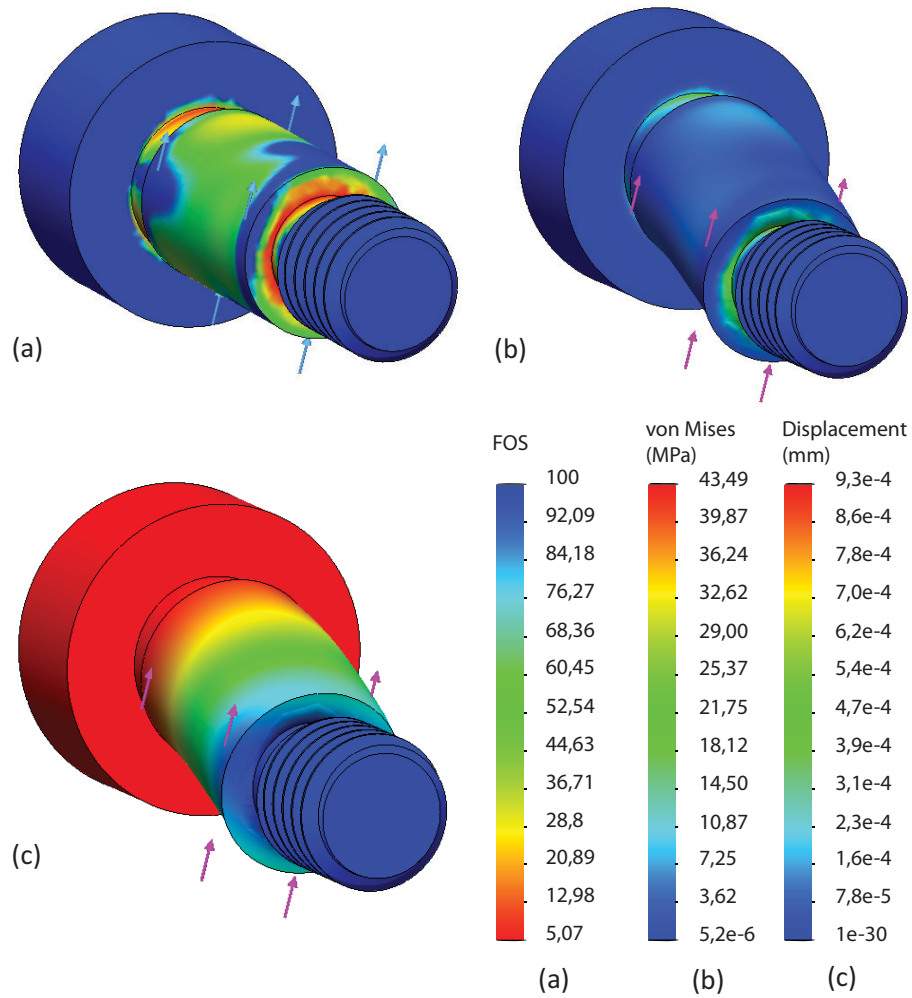
Figure 3.6: Structural analysis result of shoulder bolt of interchangeable joint for 3UPS mode. (a)Factor of safety (b)von Mises Stress [MPa] (c)Displacement [mm]

the radius of the Bowden cable driving disc. The novel tensioning mechanism is based on 2 discs sliding with respect to each other to increase the fixed cable length as shown in Figure 3.7. On the other hand, a linear series elastic actuator as shown in Figure 3.8, is designed to actuate prismatic joints of extensible links.
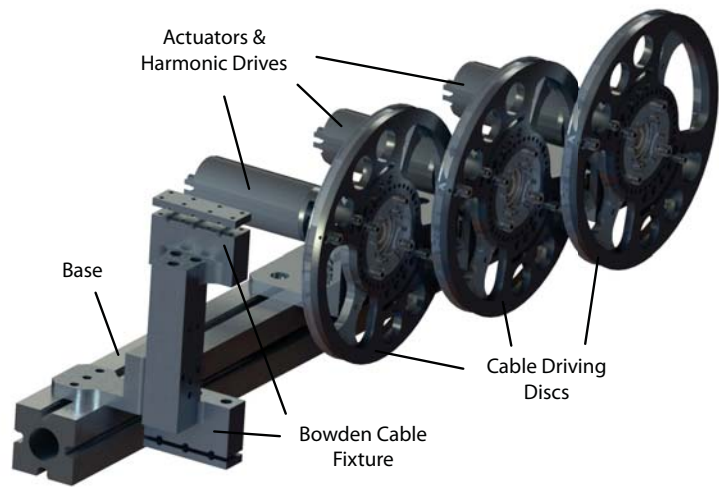
Figure 3.7: Novel remote actuation mechanism of ASSISTON-ANKLE.
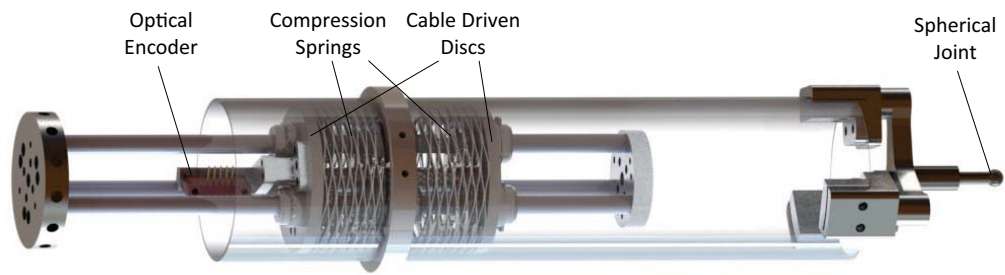
Figure 3.8: Series elastic actuator of ASSISTON-ANKLE.

Series elastic actuators control the prismatic joints of the extensible links and spherical joints transfer the motion to the end-effector. Effective RoM of the series elastic actuators are 100 mm. Wave Springs with 9.92 N/mm spring rate, are used for sensing compression in the series elastic actuator where the sensor is a linear optical encoder. To avoid bending and twisting of the series elastic actuator, 3 rods are used as the guide of the actuator. The series elastic actuator is composed of 3 discs where the actuation for both direction is imposed from the discs at the left and right ends, while the disc in the middle

is the end-effector of the actuator and rigidly connected to the spherical joints with a carbon fiber tube which also hides the interior of the actuator. The exoskeleton is rigidly connected to the shank of human via the knee brace of ASSISTON-KNEE as the connection can be seen in Figure 3.9. Then, a bearing with 165.1 mm bore diameter helps the base platform to passively rotate about the $\vec{z}$ direction of the device. Aforementioned interchangeable joints enable the revolute or universal joint for the extensible links to have a rotation with respect to the base platform. For the 3U$\underline{P}$S mode, 3 absolute magnetic rotary encoders with 10-bit resolution are used.

In total, 3 remote actuation units are required to exert motion to series elastic actuators and a single remote actuation side has a 200W graphite brushed DC motor with an optical encoder on it. A harmonic drive with 1:50 gear ratio is used for reduction and the disc that drives the Bowden cable has radius of 110 mm. In total, a single series elastic actuator can exert forces up to 191 N which creates a maximum torque of 28 Nm at the end-effector of the exoskeleton. The characteristics of the linear series elastic actuator is given in Table 3.3. The Bowden cables shields are attached to fixtures that enables easy stretching. However, comparing to ASSISTON-KNEE, bending radius of the cables smaller, which means the system has higher stick-slip friction.

It is important for the device to be wearable and portable, especially for during balance/proprioception exercises. The exoskeleton weights 4,6 kg and it is distributed over the thigh and shank of human leg. Attachment of the foot to the end-effector of the mechanism is realized strictly with the help of a shoe part of a commercial ankle orthosis. In Figure 3.10 ankle rehabilitation robot, ASSISTON-ANKLE, is worn by the user. Besides, Figure 3.11 shows

Figure 3.9: Connection of AssistOn-Knee with AssistOn-Ankle.

the first prototype of AssistOn-Ankle along with the series elastic actuator where some parts of the device is still unavailable to be assembled. Table 3.4 gives the characterization results of AssistOn-Ankle in both 3R$\underline{P}$S and 3U$\underline{P}$S modes.

Table 3.3: Characterization of Linear Series Elastic Actuator

Criteria	Data
Cont. Torque	191 N
Max. Speed	1.13 m/sec
Min. Resolvable Torque	0.12 N
Workspace	100 mm
Resolution	0.05 mm
Stiffness	9.92 N/mm

Figure 3.10: ASSISTON-ANKLE worn by the user.

Figure 3.11: First prototype of AssistOn-Ankle and its series elastic actuator.

Table 3.4: Characterization of ASSISTON-ANKLE

Criteria	R-3RPS			3UPS-RRR	
	ϕ_1	ϕ_2	Z	ϕ_1	ϕ_2
Cont. Torque/Force	28 Nm	28 Nm	500 N	22 Nm	22 Nm
Max. Speed	73 rpm	73 rpm	1 m/s	57 rpm	57 rpm
Min. Resolvable Torque/Force	0.018 Nm	0.018 Nm	0.3 N	0.012 Nm	0.012 Nm

3.5 Kinematic Verification

Kinematic test is realized by using the kinematics blocks as shown in 3.12. Inverse and forward kinematics are required to control the position and orientation of the end-effector along with force exerted on it, both in task space control and joint space control. Note that, no unique inverse kinematics for series RRR mechanism is available. So, verification only includes forward and inverse kinematics of the 3UPS manipulator. Also note that, simulation is actualized for 3UPS manipulator since kinematics of the 3RPS manipulator is more straightforward. Results of the simulation is shown in Figure 3.13. Rms error in $\vec{x}, \vec{y}$ and $\vec{z}$ is given as 2.3497, 1.9747 and 1.0259 mm, respectively.
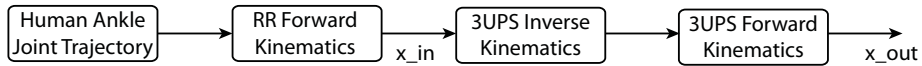

Figure 3.12: Block diagram of the simulation to verify kinematics of 3UPS manipulator.

53
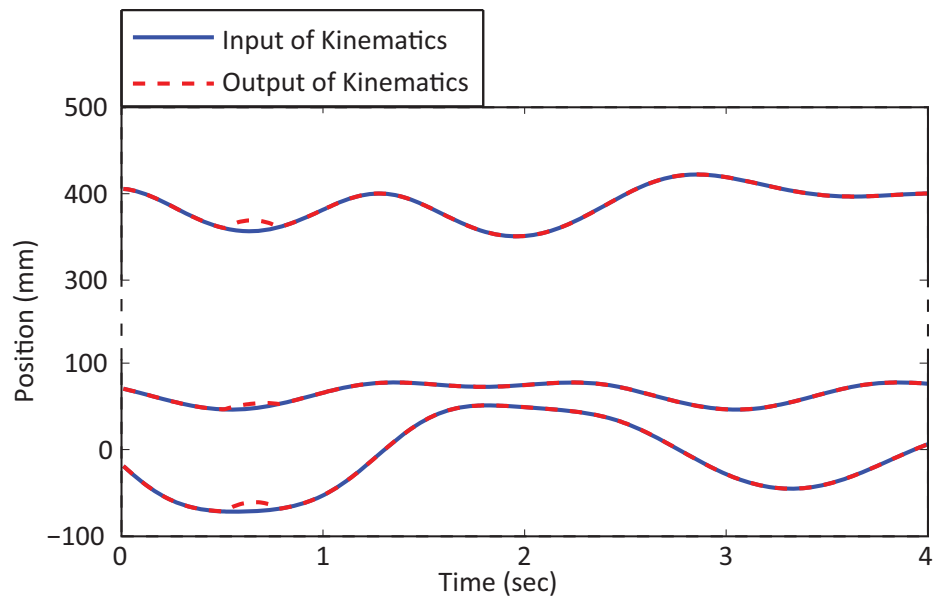
Figure 3.13: Verification of the 3U$\underline{\text{P}}$S manipulator kinematics.

Chapter IV

4 ASSISTON-LEG

This chapter explains the motivation, kinematics and design of a complete lower body exoskeleton, ASSISTON-LEG and its hip module along with kinematics of human hip and pelvis.

4.1 Kinematics of Human Hip and Pelvis Complex

Natural walking of human implies coupled movement of pelvis with hip. Ounpuu points out that during walking, motion in all rotations of pelvis and hip is observed [88]. Coupling these joints results in 6 DoF at the pelvis/hip complex. Motion in pelvis occurs with the movement of Sacrum with respect to Ilium. Ounpuu calls the rotation of pelvis in coronal plane as pelvic obliquity, in sagittal plane as pelvic tilt and in transverse plane as pelvic rotation. The maximum and minimum values that these motions can get is given in [89] and is shown in Table 4.1.

Table 4.1: Pelvic Motion Limits

Motion	Min. Rotation	Max. Rotation
Pelvic Obliquity	$-6°$	$9°$
Pelvic Tilt	$-18°$	$10°$
Pelvic Rotation	$5°$	$31°$

Motion at hip joint, on the other hand, is due to rotation of Femoral head in Acetabulum. The Iliofemoral joint in between these bones behaves as a spherical joint. The limits of motion at hip joint is given in [57] and shown in the Table 4.2. However, by coupling the movements, effective RoM can be increased. For instance, internal/external rotation range can be from $-70°$ to $90°$ as given in [90].
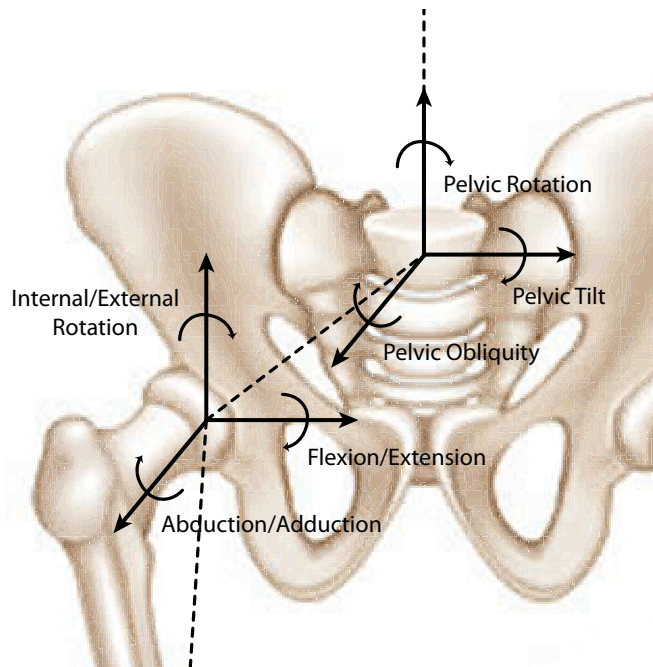
Figure 4.1: Kinematics of the human hip and pelvis

Table 4.2: Hip Motion Limits

Motion	Min. Rotation	Max. Rotation
Flexion/Extension	$-120°$	$30°$
Abduction/Adduction	$-40°$	$20°$
Internal/External Rotation	$-40°$	$50°$

Furthermore, it is convenient to investigate hip and pelvis together since as depicted in [91], motion of hip joint is coupled with motion of pelvis.

Figure 4.1 shows the modeled motions of hip and pelvis. By using the morphological data given in [92], the translation of hip joint center in the sagittal plane caused by the rotation of the pelvis, is shown in Figure 4.2 and it is seen that the workspace can be considered as a circle with radius of 60 mm. Besides, anatomy of knee and ankle joints that are also of interest are given in Chapter II and Chapter III. Ankle and knee devices presented in these chapters, support sufficient motion to promote ergonomy for walking [88].
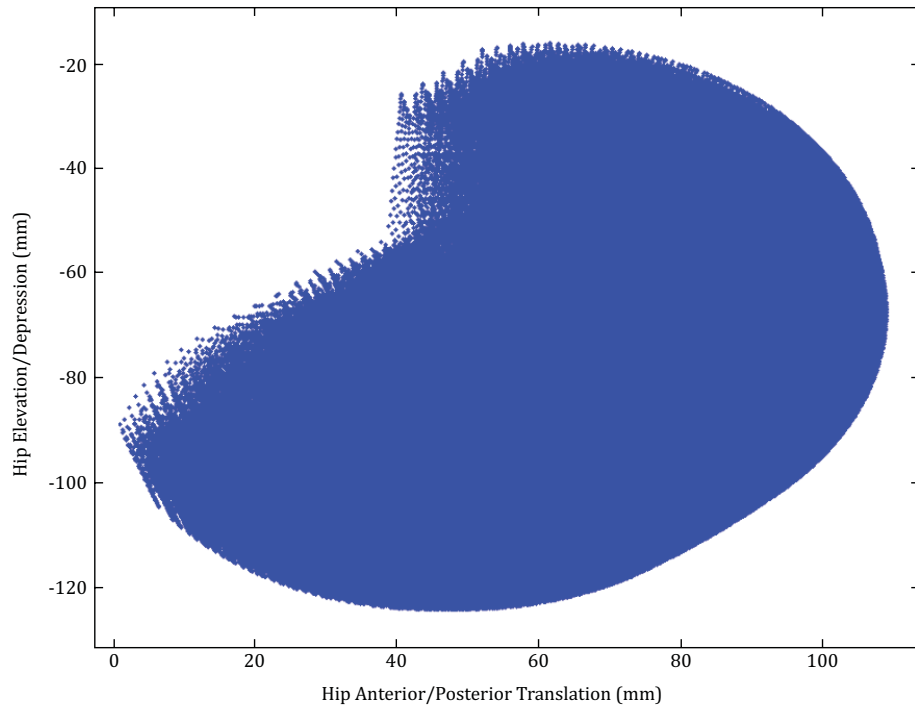
Figure 4.2: Translation of hip joint center in the sagittal plane

4.2   Design Criteria

To ensure ergonomy of the exoskeleton for complex joint structure of pelvis and hip, the device should support rotations and allow translations pas-

sively. However, the most known exoskeleton in robotic rehabilitation has only 1 DoF at hip joint [40]. A similar model of hip joint is also used by the HAL exoskeleton that models hip with only 1 DoF [5]. The kinematics of human hip and pelvis is important for natural walking of human. Devices such as [3] uses only 1 DoF at hip but the exoskeleton is supported by a gravity compensation mechanism that enables passive motions of hip and pelvis. Besides, LOPES also uses a similar mechanism that passively guides the motion of the pelvis and hip before the exoskeleton is connected to human [4]. This mechanisms enables an end-effector type support that does not involve the human limb motion and only deal with the position of the hip joint center in space. Whereas, eLEGS models hip joint with 3 DoFs that 2 of them are passive and only flexion/extension is actuated [2]. [33] on the other hand controls the abduction/adduction of hip as a difference from eLEGS. However, all devices neglect translations of hip joint with respect to pelvis. Our proposed lower body exoskeleton includes 6 DoF that 3 of them are hip rotation and translations in sagittal plane, 2 of them are abduction/adduction and internal/external rotation of hip and the last DoF is the medial/lateral translation in frontal plane. Applying these movements enables perfect match for the hip joint and allows approximation for the pelvis movements.

A 3RRP parallel manipulator is selected since it possess a singularity-free large workspace that covers human hip workspace and high torque values since it can be considered as a mechanical summer due to its parallel structure. By allowing active/passive translations in plane, it can provide ideal matching of joints and thus, ergonomy. Other motions are enabled with the help of 2 revolute and 1 prismatic joint (RPR mechanism).

4.3 Kinematics Analysis

Kinematics os ankle and knee exoskeletons have been derived in previous chapters. To obtain modular analysis of kinematics, in this section, kinematics of 3R̲RP parallel manipulator will be explained. Figure 4.3 shows the schematic representation of the 3R̲RP manipulator. On top of a based platform, 3 rotating links, A,B and C, are connected via revolute joints. The end-effector is rigidly connected to 3 rods that are connected to the rotating links with means of a revolute and a prismatic joint. This kinematics allows the end-effector to freely rotate and translate in plane.

Kinematics will not be derived in this thesis, since it is clearly explained in detail and the analytical solution is presented in [93]. Using the derived analytical Jacobian one can easily map the joint forces/torques or end-effector position/orientation to sensory data with simple equation:

$$[\dot{x} \ \dot{y} \ \dot{\theta} \ \dot{s_1} \ \dot{s_2} \ \dot{s_3}]^T = J_{3\underline{R}RP} \ [\dot{q_1} \ \dot{q_2} \ \dot{q_3}]^T \tag{19}$$

4.4 Design of ASSISTON-HIP

Design of ASSISTON-LEG is realized with use of a 3R̲RP manipulator that enables control of 2 translational and 1 rotational movement in sagittal plane at hip. Besides, the exoskeleton make use of a passive R̲PR mechanism that is seen in Figure 4.4, to allow abduction/adduction and internal/external rotation while medial/lateral translation is also supported. In total 6 DoFs are introduced to guarantee ergonomy for pelvis/hip complex with self alignment while force feedback control is applied.

This design includes capstan based actuation of R̲PR-3R̲RP mechanism
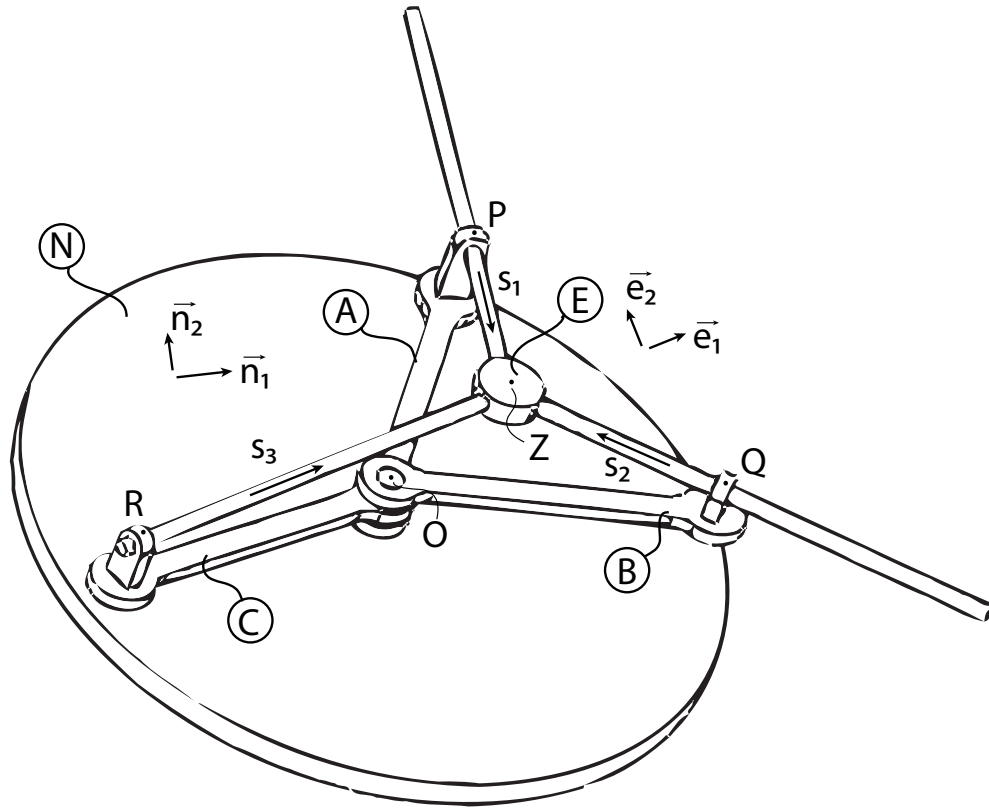
Figure 4.3: Schematic diagram of 3RRP manipulator

as a difference from the other modules in terms of the actuation. The reason for that is the weight of this module is mostly grounded and passive back-driveability is ensured with the use of low-friction capstan transmission. Thus safety of ASSISTON-HIP is ensured. The base of the exoskeleton is fixed and also tightly connected to human torso from lumbar spine which allows neglecting minimal deformations of spine and prevents kinematics of the spine to interfere with the device. On the other hand, the effector of the device is connected to ASSISTON-KNEE with the help of an adjustable-length connec-
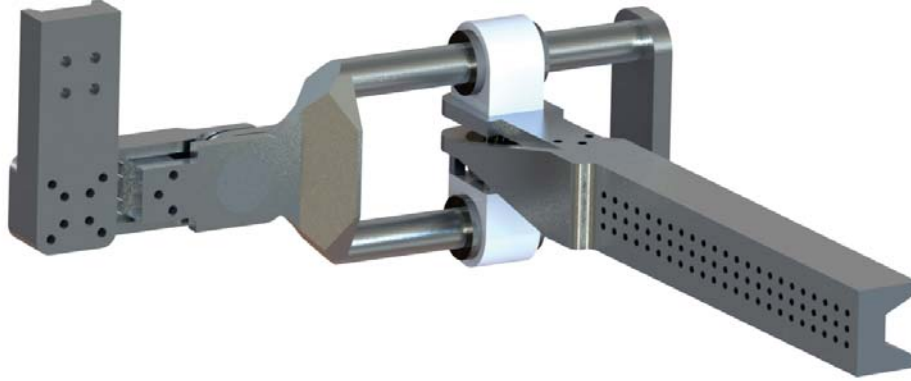
Figure 4.4: Solid model of RPR mechanism

tion part. Thus offline adjustment can be maintained for the extreme cases of extremity lengths. Besides, both 3RRP and Schmidt coupling mechanisms are self-aligning and can compensate small variations. 3RRP mechanism makes use of a workspace with diameter larger than 240 mm that covers the translational workspace of average human hip. Rotational RoM is limited to 220° due to Bowden cable actuation. The CAD model for the 3RRP mechanism is given in Figure 4.5. The passive revolute and prismatic joints also has mechanical limits for motion. The joint that enables internal/external rotation of hip has a limit of $\mp 70°$, the abduction/adduction enabling one has a limit of $\mp 240°$ and the slider that enables medial/lateral translation has a motion range of 75 mm. To reduce the gap of the bearings and structural stiffness, double bearings are used for these passive revolute joints.

Design of RPR-3RRP mechanism, unlike AssistOn-Knee, is symmetric and can be used for both legs. Yet, AssistOn-Knee needs orthosis that is for particular use of specified leg to be connected to human. Thus, use of
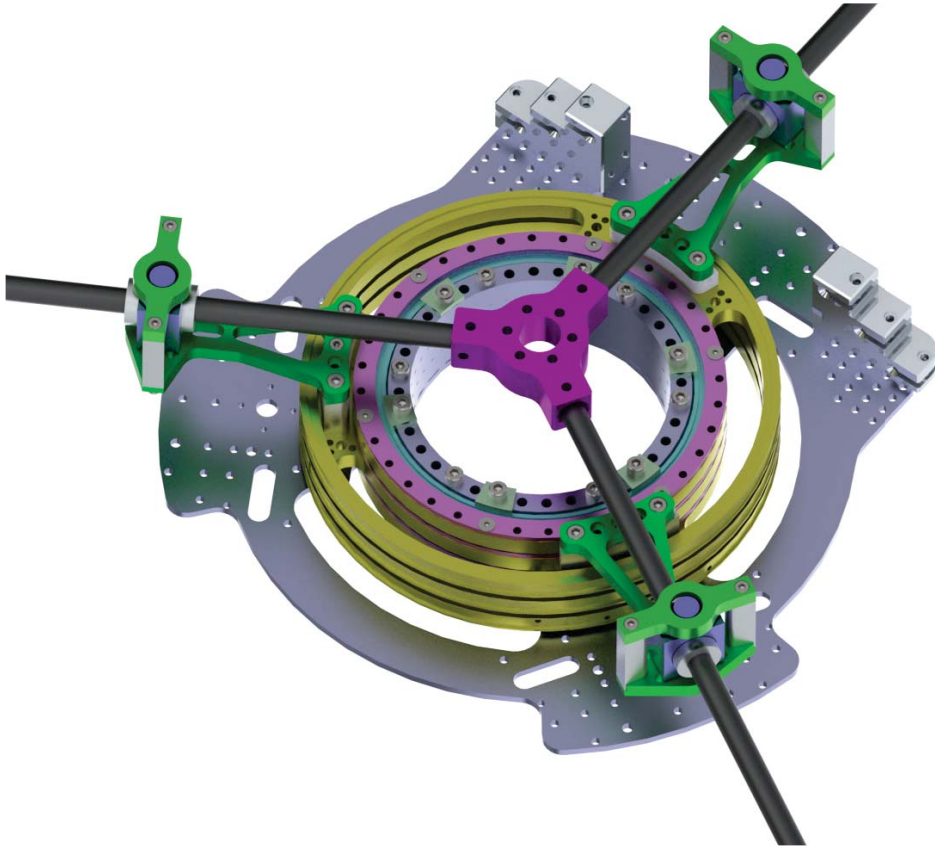
Figure 4.5: Solid model of 3RRP mechanism as proposed in [6]

ASSISTON-LEG is limited to the specified leg and with use of commercial orthosis for both legs, ASSISTON-LEG can be used as a whole lower body exoskeleton.

The workspace of the exoskeleton at actuated joints of pelvis/hip complex in sagittal plane is given in Table 4.3. Passive joints are free to rotate within mechanical limitations and all joints are capable of covering human workspace.

As the actuation mechanism, 2 level capstan mechanism is used to actuate

Table 4.3: RoM of controlled motions for hip/pelvis complex in sagittal plane

Movement	Flexion	Extension	Elevation/Depression	Anterior/Posterior Trans.
Amplitude	170°	50°	120/120 mm	120/120mm
Range		220°	240 mm	240 mm

3<u>R</u>RP mechanism. 250W graphite brushed DC motors with optical encoder is instrumented in order to actuate a capstan mechanism with 1:5 reduction and this mechanism actuates a second capstan mechanism with 1:5.5 gear reduction. In total, 1:27.5 gear reduction is maintained. Thanks to the mechanical summer feature of 3<u>R</u>RP mechanism, continuous torque of 58.6 Nm can be supported for flexion/extension and for translations in the sagittal plane, the mechanism can exert up to 262.5 N continuous force. To measure the orientation of <u>RPR</u> mechanism, optical rotary encoders are used. The CAD model of ASSISTON-HIP, is worn by the user as given in Figure 4.6.

4.4.1 Structural Analysis

Structural simulations of the 3<u>R</u>RP manipulator is performed with finite element analysis tool embedded in SolidWorks Simulation CAD-embedded analysis (Cosmos). Corresponding results are given in Figure 4.7. The materials used in the design is made of aluminum with yield strength of 200 MPa. The assembly is investigated rather than single parts. However, relative motion of bodies are defined using bearings. The fixture is added to the base platform where the bearings of bodies A,B and C are connected. Whereas, the torque input of 250 N along both x and y direction in the plane is introduced to end-effector. Besides, 45 Nm of torque and 15 N force perpendicular to the xy-plane added. In total, introduced external forces/torques exceed the limits that the manipulator can apply.
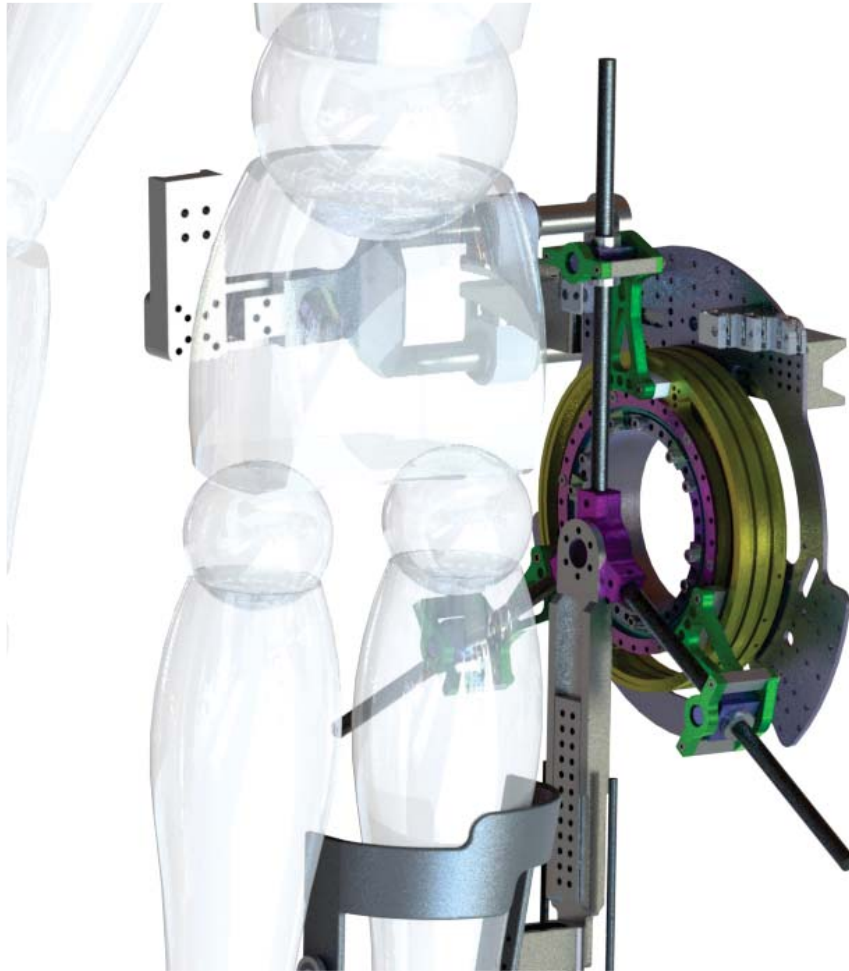
Figure 4.6: ASSISTON-HIP worn by the user

Meshing is done using 4 points Jacobian points with size of 2.5 mm for larger parts and 0.6 mm for smaller parts. Corresponding results shows that maximum stress that the coupling is composed to, is 47 MPa, concentrated on the extensible links and their connections with bodies, A,B and C. Minimum observed safety factor is 2,69 which is sufficient for use of the device. Besides, maximum displacement is 0.6 millimeters.
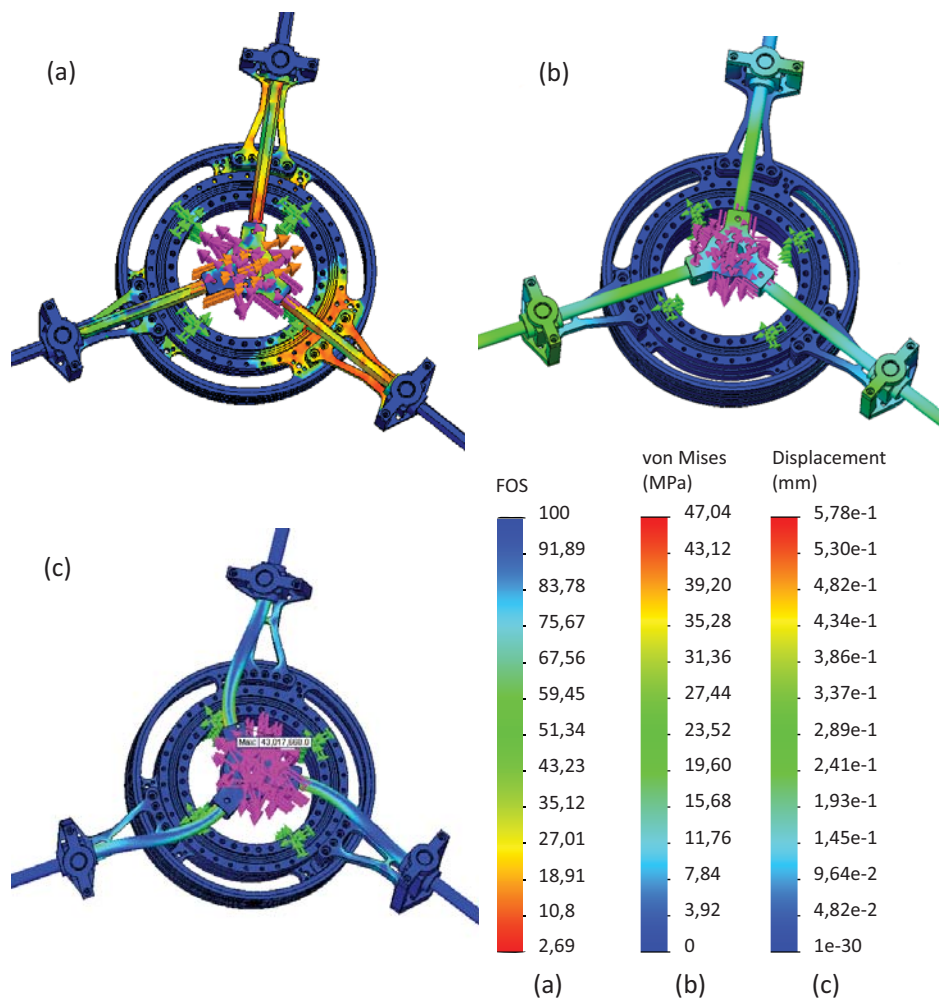
Figure 4.7: Structural analysis result of 3R̲RP manipulator. (a)Factor of safety (b)von Mises Stress [MPa] (c)Displacement [mm]

Chapter V

5 Conclusion & Future Works

Kinematics of ASSISTON-KNEE, ASSISTON-ANKLE and ASSISTON-HIP are presented along with design details and Bowden cable-driven series elastic actuation of distal joints of ASSISTON-LEG. Experimental characterization results and feasibility studies on healthy volunteers for ASSISTON-KNEE are also provided. Safety of the device is ensured with impact resistant structure of series elasticity and passive backdriveability. Design of the ASSISTON-LEG is realized with use of complex and sufficient kinematics that can provide self-alignment and thanks to the self-aligning feature of the ASSISTON-LEG, perfect match between human joint axes and exoskeleton axes are maintained that sustains ergonomy and comfort throughout rehabilitation therapies. Besides, setup time is significantly shortened in ASSISTON-LEG, comparing to existing devices in literature.

Due to time and financial limitations, ASSISTON-HIP has not been manufactured yet. Its implementation and characterization are among our planned future work. Besides, controlling the linear series elastic actuators of ASSISTON-ANKLE is considered in the future work. Our future work also includes larger scale human subject experiments and tracking of human gait with/without ASSISTON-LEG to verify that the devices does not interfere with natural walking gait of its users.

References

[1] Robert Riener, Lars Lünenburger, and Gery Colombo. Human-Centered Robotics Applied to Gait Training and Assessment. *Veterans Admin. Journal of Rehabilitation Research and Development*, pages 679–694, 2006.

[2] Katherine A Strausser and H Kazerooni. The development and testing of a human machine interface for a mobile medical exoskeleton. In *Intelligent Robots and Systems (IROS), 2011 IEEE/RSJ International Conference on*, pages 4911–4916. IEEE, 2011.

[3] Sai K. Banala, Seok Hun Kim, Sunil K. Agrawal, and John P. Scholz. Robot Assisted Gait Training With Active Leg Exoskeleton (ALEX). *IEEE Transactions on Neural Systems and Rehabilitation Engineering*, 17:2–8, 2009.

[4] Jan Frederik Veneman. *Design and evaluation of the gait rehabilitation robot LOPES*. PhD thesis, Enschede, December 2007.

[5] Hiroaki Kawamoto, Tomohiro Hayashi, Takeru Sakurai, Kiyoshi Eguchi, and Yoshiyuki Sankai. Development of single leg version of hal for hemiplegia. In *Engineering in Medicine and Biology Society, 2009. EMBC 2009. Annual International Conference of the IEEE*, pages 5038–5043. IEEE, 2009.

[6] Mustafa Yalcin and Volkan Patoglu. Kinematics and design of assiston-se: A self-adjusting shoulder-elbow exoskeleton. In *IEEE International Conference on Biomedical Robotics and Biomechatronics*, pages 1579–1585, 2012.

[7] Global burden of stroke. `http://www.who.int/cardiovascular_diseases/en/cvd_atlas_15_burden_stroke.pdf`.

[8] Description of physical therapy. Technical report, World Confederation for Physical Therapy, 2011.

[9] Cathrin Batefisch, Horst Hummelsheim, Petra Denzler, and Karl-Heinz Mauritz. Repetitive training of isolated movements improves the outcome of motor rehabilitation of the centrally paretic hand. *Journal of the Neurological Sciences*, 130(1):59–68, 1995.

[10] Gert Kwakkel, Robert C Wagenaar, Jos WR Twisk, Gustaaf J Lankhorst, and Johan C Koetsier. Intensity of leg and arm training after primary middle-cerebral-artery stroke: a randomised trial. *The Lancet*, 354(9174):191–196, 1999.

[11] A Sunderland, D J Tinson, E L Bradley, D Fletcher, R Langton Hewer, and D T Wade. Enhanced physical therapy improves recovery of arm function after stroke. a randomised controlled trial. *Journal of Neurology, Neurosurgery and Psychiatry*, 55(7):530–535, 1992.

[12] Nestor A. Bayona, Jamie Bitensky, Katherine Salter, and Robert Teasell. The role of task-specific training in rehabilitation therapies. *Topics in Stroke Rehabilitation*, 12(3):58–65, June 2005.

[13] G. B. Prange, M. J. Jannink, C. G. Groothuis-Oudshoorn, H. J. Hermens, and M. J. Ijzerman. Systematic review of the effect of robot-aided therapy on recovery of the hemiparetic arm after stroke. *Journal of rehabilitation research and development*, 43(2):171–184, 2006.

[14] Gert Kwakkel, Boudewijn J. Kollen, and Hermano I. Krebs. Effects of robot-assisted therapy on upper limb recovery after stroke: A systematic review. *Neurorehabilitation and Neural Repair*, 22(2):111–121, 2008.

[15] Jan Mehrholz, Thomas Platz, Joachim Kugler, and Marcus Pohl. Electromechanical and robot-assisted arm training for improving arm function and activities of daily living after stroke. *Stroke*, 40:e292–e293, 2009.

[16] Kati Nykanen. The effectiveness of robot-aided upper limb therapy in stroke rehabilitation: A systematic review of randomized controlled studies. Master's thesis, University of Jyväskylä, Institute of Health Sciences, Physiotherapy, 2010.

[17] N. Hogan, H.I. Krebs, J. Charnnarong, P. Srikrishna, and A. Sharon. Mit-manus: a workstation for manual therapy and training. i. In *IEEE International Workshop on Robot and Human Communication*, pages 161–165, Sep 1992.

[18] A. Frisoli, F. Rocchi, S. Marcheschi, A. Dettori, F. Salsedo, and M. Bergamasco. A new force-feedback arm exoskeleton for haptic interaction in virtual environments. In *Eurohaptics Conference, Symposium on Haptic Interfaces for Virtual Environment and Teleoperator Systems. World Haptics 2005. First Joint*, pages 195–201, March 2005.

[19] R. Ekkelenkamp, J. Veneman, and H. van der Kooij. Lopes: a lower extremity powered exoskeleton. In *IEEE International Conference on Robotics and Automation*, pages 3132–3133, April 2007.

[20] B. Vanderborght, N.G. Tsagarakis, C. Semini, R. Van Ham, and D.G. Caldwell. Maccepa 2.0: Adjustable compliant actuator with stiffening characteristic for energy efficient hopping. In *IEEE International Conference on Robotics and Automation, ICRA*, pages 544–549, May 2009.

[21] Furui Wang, D.E. Barkana, and N. Sarkar. Impact of visual error augmentation when integrated with assist-as-needed training method in robot-assisted rehabilitation. *IEEE Transactions on Neural Systems and Rehabilitation Engineering*, 18(5):571–579, Oct 2010.

[22] Aykut Cihan Satici, Ahmetcan Erdogan, and Volkan Patoglu. A multilateral rehabilitation system. *Turkish Journal of Electrical Engineering and Computer Sciences*, 19(5):715–723, 2011.

[23] A. Erdogan and V. Patoglu. Slacking prevention during assistive contour following tasks with guaranteed coupled stability. In *IEEE/RSJ International Conference on Intelligent Robots and Systems (IROS), 2012*, pages 1587–1594, Oct.

[24] M. Cenciarini and A. M. Dollar. Biomechanical considerations in the design of lower limb exoskeletons. In *IEEE International Conference on Rehabilitation Robotics (ICORR)*, pages 1–6, July 2011.

[25] A. Schiele and F.C.T. van der Helm. Kinematic design to improve ergonomics in human machine interaction. *IEEE Transactions on Neural Systems and Rehabilitation Engineering*, 14(4):456–469, Dec. 2006.

[26] A.H.A. Stienen, E.E.G. Hekman, F.C.T. van der Helm, and H. van der Kooij. Self-aligning exoskeleton axes through decoupling of joint rota-

tions and translations. *IEEE Transactions on Robotics*, 25(3):628–633, June 2009.

[27] P. S. Lum, S. Mulroy, R. L. Amdur, P. Requejo, B. I. Prilutsky, and A. W. Dromerick. Gains in upper extremity function after stroke via recovery or compensation: Potential differential effects on amount of real-world limb use. *Topics in Stroke Rehabilitation*, 16(4):237–253, 2009.

[28] D.G. Caldwell, C. Favede, and N. Tsagarakis. Dextrous exploration of a virtual world for improved prototyping. In *IEEE International Conference on Robotics and Automation*, volume 1, pages 298–303, May 1998.

[29] C. Carignan, M. Liszka, and S. Roderick. Design of an arm exoskeleton with scapula motion for shoulder rehabilitation. In *12th International Conference on Advanced Robotics, ICAR '05*, pages 524–531, July 2005.

[30] T. Nef, M. Guidali, and R. Riener. Armin iii - arm therapy exoskeleton with an ergonomic shoulder actuation. *Applied Bionics and Biomechanics*, 2(6):127–142, 2009.

[31] Jaipur knee. http://remotiondesigns.org/jaipurknee.html.

[32] V. Cai, Ph. Bidaud, V. Hayward, and F. Gosselin. Design of self-adjusting orthoses for rehabilitation. In *Proceedings of the 14th IASTED International Conference on Robotics and Applications*, pages 215–223, 2009.

[33] Hian Kai Kwa, Jerryll H Noorden, Matthew Missel, Travis Craig, Jerry E Pratt, and Peter D Neuhaus. Development of the ihmc mo-

bility assist exoskeleton. In *Robotics and Automation, 2009. ICRA'09. IEEE International Conference on*, pages 2556–2562. IEEE, 2009.

[34] Jacob Apkarian, Stephen Naumann, and Bonnie Cairns. A three-dimensional kinematic and dynamic model of the lower limb. *Journal of Biomechanics*, 22(2):143–155, 1989.

[35] L. Blankevoort and R. Huiskes. Validation of a three-dimensional model of the knee. *Journal of Biomechanics*, 29(7):955–961, 1996.

[36] J. Bellmans, J. Bellemans, and M. D. Ries. *Total Knee Arthroplasty: A Guide to Get Better Performance*, pages 130–134. Springer Berlin Heidelberg, hardbound edition, July 2005.

[37] Kok-Meng Lee and Jiajie Guo. Kinematic and dynamic analysis of an anatomically based knee joint. *Journal of Biomechanics*, 43(7):1231–1236, 2010.

[38] Andy Williams and Martin Logan. Understanding tibio-femoral motion. *The Knee*, 11(2):81–88, 2004.

[39] Nancy Hamilton, Wendi Weimar, and Kathryn Luttgens. *Kinesiology: Scientific Basis of Human Motion*. McGraw-Hill, New York, NY, 12 edition, 2012.

[40] Saso Jezernik, Gery Colombo, Thierry Keller, Hansruedi Frueh, and Manfred Morari. Robotic Orthosis Lokomat: A Rehabilitation and Research Tool. *Neuromodulation*, 6:108–115, 2003.

[41] Adam B. Zoss, H. Kazerooni, and Andrew Chu. Biomechanical design of the Berkeley lower extremity exoskeleton (BLEEX). *IEEE-ASME Transactions on Mechatronics*, 11:128–138, 2006.

[42] Fabrizio Sergi, Dino Accoto, Giorgio Carpino, Nevio Luigi Tagliamonte, and Eugenio Guglielmelli. Design and characterization of a compact rotary series elastic actuator for knee assistance during overground walking. In *IEEE RAS & EMBS International Conference on Biomedical Robotics and Biomechatronics*, pages 1931–1936, June 2012.

[43] Nikos C. Karavas, Nikolaos G. Tsagarakis, and Darwin G. Caldwell. Design, modeling and control of a series elastic actuator for an assistive knee exoskeleton. In *IEEE RAS & EMBS International Conference on Biomedical Robotics and Biomechatronics*, pages 1813–1819, June 2012.

[44] Jerry E. Pratt, Benjamin T. Krupp, Christopher J. Morse, and Steven H. Collins. The roboknee: an exoskeleton for enhancing strength and endurance during walking. In *IEEE International Conference on Robotics and Automation, ICRA'04*, pages 2430–2435, April 2004.

[45] James S. Sulzer, Ronald A. Roiz, Michael A. Peshkin, and James L. Patton. A highly backdrivable, lightweight knee actuator for investigating gait in stroke. *IEEE Transactions on Robotics*, 25(3):539–548, 2009.

[46] K. J. Kim, M. S. Kang, Y. S. Choi, J. Han, and C. Han. Conceptualization of an exoskeleton continuous passive motion (cpm) device using a link structure. In *IEEE International Conference on Rehabilitation Robotics (ICORR)*, pages 1–6, June 2011.

[47] D. Wang, J. Guo, K. M. Lee, C. Yang, and H. Yu. An adaptive knee joint exoskeleton based on biological geometries. In *IEEE International Conference on Robotics and Automation (ICRA)*, pages 1386–1391, May 2011.

[48] L. E. Amigo, A. Casals, and J. Amat. Design of a 3-dof joint system with dynamic servo-adaptation in orthotic applications. In *IEEE International Conference on Robotics and Automation (ICRA)*, pages 3700–3705, May 2011.

[49] Mehmet Alper Ergin and Volkan Patoglu. A self-adjusting knee exoskeleton for robot-assisted treatment of knee injuries. In *IEEE/RSJ International Conference on Intelligent Robots and Systems (IROS)*, pages 4917–4922, Sept. 2011.

[50] Viet Anh Dung Cai, Philippe Bidaud, Vincent Hayward, Florian Gosselin, and Eric Desailly. Self-adjusting, isostatic exoskeleton for the human knee joint. In *Annual International Conference of the IEEE Engineering in Medicine and Biology Society, EMBC*, pages 612–618, Aug-Sept 2011.

[51] Besir Celebi, Mustafa Yalcin, and Volkan Patoglu. AssistOn-Knee: a self-aligning knee exoskeleton. In *IEEE/RSJ International Conference on Intelligent Robots and Systems (IROS)*, Nov. 2013.

[52] Schmidt-kupplung: Specialist for compact precision couplings, July 2013.

[53] Richard Schmidt. Coupling, Feb 1974.

[54] J. W. Sensinger and R. F. ff. Weir. Improvements to series elastic actuators. In *IEEE/ASME International Conference on Mechatronic and Embedded Systems and Applications*, 2006.

[55] G. A. Pratt and M. M. Williamson. Series elastic actuators. In *IEEE International Conference on Intelligent Robots and Systems*, 1995.

[56] Robert W. Horst. A bio-robotic leg orthosis for rehabilitation and mobility enhancement. In *Annual International Conference of the IEEE Engineering in Medicine and Biology Society*, pages 5030–5033, 2009.

[57] Cynthia C. Norkin and D. Joyce White. *Measurement Of Joint Motion: A Guide To Goniometry*. FA Davis Company, 4 edition, 2009.

[58] J.S.Dai, T. Zhao, and C. Nester. Sprained ankle physiotherapy based mechanism synthesis and stiffness analysis of a robotic rehabilitation device. In *Autonomous Robots*, volume 16, 2004.

[59] J. Yoon and J. Ryu. Design, fabrication, and evaluation of a new haptic device using a parallel mechanism. *IEEE Transactions on Mechatronics*, 6(3):221–233, 2001.

[60] C. E. Syrseloudis, I. Z. Emiris, C. N. Maganaris, and T. E. Lilas. Design framework for a simple robotic ankle evaluation and rehabilitation device. In *International IEEE EMBS Conference*, 2008.

[61] R.E. Isman and V.T. Inman. Anthropometric studies of the human foot and ankle. *Bulletin of Prosthesis Research*, 10-11:97–129, 1969.

[62] J. Yoon, J. Ryu, and K. Lim. A novel reconfigurable ankle rehabilitation robot for various exercise modes. *Journal of Robotic Systems (Currently Journal of Field Robotics)*, 22(1):15–33, 2006.

[63] USA, Department of Defence. Military handbook anthropometry of u.s. military personnel (metric), February 1991. DOD-HDBK-743A.

[64] A. Agrawal, S. K. Banala, S. K. Agrawal, and S. A. Binder-Macleod. Design of a two degree-of-freedom ankle-foot orthosis for robotic rehabilitation. In *Proceedings of the IEEE International Conference on Rehabilitation Robotics*, pages 41–44, 2005.

[65] M. Girone, G. Burdea, and M. Bouzit. The Rutgers Ankle orthopedic rehabilitation interface. In *Proceedings of the ASME Haptics Symposium*, volume 67, pages 305–312, 1999.

[66] M. Girone, G. Burdea, M. Bouzit, V. Popescu, and J.E. Deutsch. Orthopedic rehabilitation using the Rutgers Ankle interface. In *Proceedings of Virtual Reality Meets Medicine 2000*, pages 89–95, 2000.

[67] J. E. Deutsch, J. Latonio, G. Burdea, and R. Boian. Rehabilitation of musculoskeletal injuries using the Rutgers Ankle haptic interface: Three case reports. In *Eurohaptics Conference*, pages 11–16, 2001.

[68] J.E. Deutsch, J. Latonia, G. Burdea, and R. Boian. Post-stroke rehabilitation with the Rutgers Ankle system: A case study. *PRESENCE*, 10(4):416–430, 2001.

[69] Daniel P Ferris, Keith E Gordon, Gregory S Sawicki, and Ammanath Peethambaran. An improved powered ankle–foot orthosis using proportional myoelectric control. *Gait & posture*, 23(4):425–428, 2006.

[70] Robin Chin, Elizabeth Hsiao-Wecksler, Eric Loth, Géza Kogler, Scott Manwaring, Serena Tyson, K Alex Shorter, and Joel Gilmer. A pneumatic power harvesting ankle-foot orthosis to prevent foot-drop. *Journal of neuroengineering and rehabilitation*, 6(1):19, 2009.

[71] A. Roy, H. I. Krebs, S. L. Patterson, T. N. Judkins, I. Khanna, L. W. Forrester, R. M. Macko, and N. Hogan. Measurement of human ankle stiffness using the Anklebot. In *Proceedings of the IEEE International Conference on Rehabilitation Robotics*, pages 356–363, 2007.

[72] J. Yoon and J. Ryu. A novel reconfigurable ankle/foot rehabilitation robot. In *IEEE International Conference on Robotics and Automation*, 2005.

[73] X. Kong and C. M. Gosselin. Type synthesis of 3-DoF spherical parallel manipulators based on screw theory. In *ASME Design Engineering Technical Conferences*, 2002.

[74] M. Karouia and J. M. Herve. A family of novel orinetational 3-DoF parallel robots. In *CISM-IFToMM Symposium on Robot Design, Dynamics, and Control*, pages 359–368, 2002.

[75] R. Di Gregorio. Kinematics of a new spherical parallel manipulator with three equal legs: The 3-URC wrist. *Journal of Robotic Systems*, 18(5):213–219, 2001.

[76] I. A. Bonev and C. M. Gosselin. Singularity loci of spherical parallel mechanisms. In *IEEE International Conference on Robotics and Automation*, pages 2957–2962, 2005.

[77] K. M. Lee and D. K. Shah. Kinematic analysis of a three degrees-of-freedom in-parallel actuated manipulator. *IEEE Transactions on Robotics and Automation*, 4(3):354–360, 1988.

[78] C. H. Liu and S. Cheng. Direct singular positions of 3RPS parallel manipulators. *ASME Journal of Mechanical Design*, (126):1006–1016, 2004.

[79] A. Gupta and M. K. O'Malley. Design of a haptic arm exoskeleton for training and rehabilitation. *IEEE Transactions on Mechatronics*, 11(3), 2006.

[80] A. Gupta, V. Patoglu, M. K. O'Malley, and C. M. Burgar. Design, control and performance of RiceWrist: A force feedback wrist exoskeleton for rehabilitation and training. *International Journal of Robotics Research, Special Issue on Machines for Human Assistance and Augmentation*, 27(2):233–251, 2008.

[81] R. Unal and V. Patoglu. Optimal dimensional synthesis of force feedback lower arm exoskeletons. In *IEEE International Conference on Biomedical Robotics and Biomechatronics*, 2008.

[82] R. Unal and V. Patoglu. Optimal dimensional synthesis of a dual purpose haptic exoskeleton. In *Lecture Notes in Computer Science, Vol. 5024, Springer*, 2008.

[83] A. K. Dashand I. M. Chen, S. H. Yeo, and G. Yang. Task-oriented configuration design for reconfigurable parallel manipulators. *International Journal of Computer Integrated Manufacturing*, 18(7):615–634, 2005.

[84] R. M. Setchi and N. Lagos. Reconfigurability and reconfigurable manufacturing systems state-of-the-art review. In *IEEE International Conference on Industrial Informatics*, pages 529–535, 2004.

[85] M. Nourelfath, D. Ait-kadi, and I. Soro. Optimal design of reconfigurable manufacturing systems. In *IEEE International Conference on Systems, Man and Cybernetics*, 2002.

[86] M.M. Mirbagheri, C. Tsao, E. Pelosin, and W.Z. Rymer. Therapeutic robotics: A technology push. In *Proceedings of the IEEE*, volume 94, pages 1727–1738, 2006.

[87] A. Erdogan, A. C. Satici, and V. Patoglu. Reconfigurable force feedback ankle exoskeleton for physical therapy. In *ASME/IFToMM International Conference on Reconfigurable Mechanisms and Robots*, 2009.

[88] Sylvia Ounpuu. The biomechanics of walking and running. *Clinics in Sports Medicine*, 13(4):843–863, 1994.

[89] Isao Asayama, Yuichiro Akiyoshi, Masatoshi Naito, and Masamitsu Ezoe. Intraoperative pelvic motion in total hip arthroplasty. *The Journal of arthroplasty*, 19(8):992–997, 2004.

[90] Paul E Hughes, Jim C Hsu, and Matthew J Matava. Hip anatomy and biomechanics in the athlete. *Sports medicine and arthroscopy review*, 10(2):103–114, 2002.

[91] Anthony G Schache, Peter D Blanch, and Anna T Murphy. Relation of anterior pelvic tilt during running to clinical and kinematic measures of hip extension. *British Journal of Sports Medicine*, 34(4):279–283, 2000.

[92] David Gentry Steele. *The anatomy and biology of the human skeleton.* Texas A&M University Press, 1988.

[93] M.A. Ergin and V. Patoglu. Assiston-se: A self-aligning shoulder-elbow exoskeleton. In *Robotics and Automation (ICRA), 2012 IEEE International Conference on,* pages 2479–2485, 2012.